ACS OMEGA

Open Access

http://pubs.acs.org/journal/acsodf

Article

Bioinformatics Analysis and Experimental Verification Define Different Angiogenesis Subtypes in Endometrial Carcinoma and Identify a Prognostic Signature

Qi Zhang, Yuwei Yao, Zhicheng Yu, Ting Zhou, Qian Zhang, Haojia Li, Jun Zhang, Sitian Wei, Tangansu Zhang,* and Hongbo Wang*

Cite This: *ACS Omega* 2024, 9, 26519−26539

Read Online

ACCESS | Metrics & More | Article Recommendations | Supporting Information

ABSTRACT: Increasing evidence indicates that peripheral blood vessels play a pivotal role in regulating tumor growth with the presence of new blood vessels facilitating tumor growth and metastasis. Nevertheless, the impact of specific molecule-mediated angiogenesis on the tumor immune microenvironment (TIME) and individual prognosis of uterine corpus endometrial carcinoma (UCEC) remains uncertain. The transcriptome information on 217 prognostic angiogenesis-related genes was integrated, and the angiogenesis patterns of 506 UCEC patients in The Cancer Genome Atlas (TCGA) cohort were comprehensively evaluated. We identified five angiogenic subtypes, namely, EC1, EC2, EC3, EC4, and EC5, which differed significantly in terms of prognosis, clinicopathological features, cancer hallmarks, genomic mutations, TIME patterns, and immunotherapy responses. Additionally, an angiogenesis-related prognostic risk score (APRS) was constructed to enable an individualized comprehensive evaluation. In multiple cohorts, APRS demonstrated a powerful predictive ability for the prognosis of UCEC patients. Likewise, APRS was confirmed to be associated with clinicopathological features, genomic mutations, cancer hallmarks, and TIME patterns in UCEC patients. The predictability of APRS for immune checkpoint inhibitor (ICI) therapy was also salient. Subsequently, the expression levels of four angiogenesis-related hub genes were verified by qRT-PCR, immunohistochemistry, and single-cell sequencing data analysis. The effects of four representative genes on angiogenesis were validated by Wound-Healing and Transwell assays, tube formation assay in vitro, and tumor xenograft model in vivo. This study proffered a new classification of UCEC patients based on angiogenesis. The established APRS may contribute to individualized prognosis prediction and immunotherapy selections that are better suited for UCEC patients.

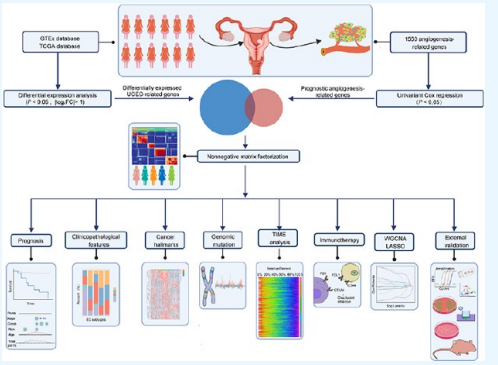

1. INTRODUCTION

Angiogenesis is the process by which pre-existing vascular systems give rise to new blood vessels. The breakdown of the extracellular matrix (ECM) and basal layer, the migration and proliferation of endothelium cells, the germination and branching of new blood vessels, and the maturity of blood vessels are all part of this intricate multistep process.[1,2] Studies have shown that protein tyrosine phosphatase PTPRJ/DEP-1 helps regulate the Notch signaling pathway and sprouting angiogenesis. BMP2 and BMP6 synergistically regulate VEGF-induced endothelial cell germination by regulating VEGFR, Notch, or TAZ-Hippo signals and promote angiogenesis in vivo.[3] Angiogenesis is a biological process involving wound healing, fetal growth and development, and endometrial proliferation.[4] An "angiogenic switch"—a process where pro- and antiangiogenic factors are out of balance—can result in a number of clinical diseases, including inflammation, restenosis, and tumors.[5] Tumors require vascular beds to grow above 1−2 mm, as they are typically highly metabolized. These new blood vessels promote the spread of metastasis and interfere with immune responses due to their frequent deformation and leakage. One of the main elements in the growth and development of tumors is angiogenesis. Evidence suggests that the YAP/RUNX2/SRSF1 axis regulates VEGF165 secretion and neuroblastoma angiogenesis in response to ECM stiffness.[6] One important regulator of tumor angiogenesis and vascular integrity is endothelial TRPV4. TRPV deficiency promotes tumor angiogenesis, growth, and metastasis.[7] The role of Agrin as an external regulator of angiogenesis and the accumulation of Agrin and perlecan in tumor ECM control tumor growth and metastasis.[8] So far, angiogenesis inhibitors have been extensively studied. The discovery of angiogenesis inhibitors provides hope

Received: March 29, 2024
Revised: May 21, 2024
Accepted: May 27, 2024
Published: June 10, 2024

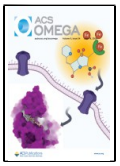

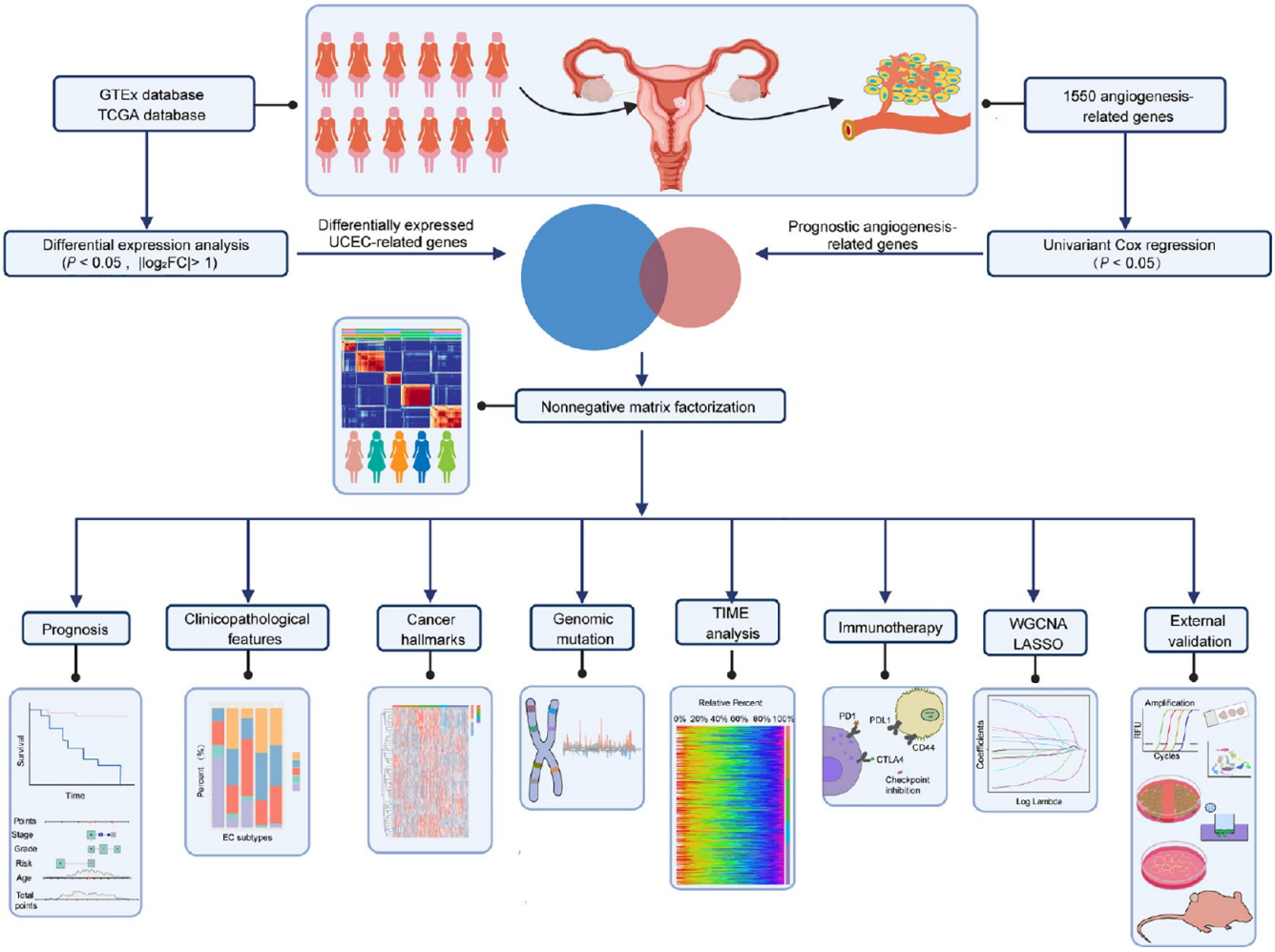

Figure 1. Overall flow diagram of this study.

for reducing cancer morbidity and mortality, but satisfactory results have not yet been achieved. Therefore, exploring the role of angiogenesis in tumors is conducive to the understanding of tumor incidence, metastasis, prognosis prediction, and the customization of personalized treatment options.

Uterine corpus endometrial carcinoma (UCEC) is the sixth most prevalent cancer that is a risk to women' health and the second most common gynecological tumor after cervical cancer. With 417,000 new cases and 97,000 deaths from gynecological cancer in 2020,[9] UCEC is the fourth leading cause of death globally.[10] The fraction of patients with early stage UCEC who survive for five years overall is more than 75%. Whereas 10−15% of patients with UCEC present with advanced-stage disease, and their prognosis is poor.[11] Although patients with early stage diseases can be treated by surgery and adjuvant therapy, there is no effective treatment for advanced diseases. Therefore, it is vitally crucial to identify workable markers that can foresee the result of immunotherapy and divide patients with different traits into different groups. Predictive biomarker-based tumor medications typically receive Food and Drug Administration (FDA) approval more swiftly due to their higher likelihood of benefiting patients.

Based on the comprehensive analysis of angiogenesis, five subtypes of angiogenesis identified in this study were recognized with different prognosis, clinicopathological features, hallmark characteristics, genomic mutations, tumor immune microenvironment (TIME) patterns, and immunotherapy responses. The strong predictive value was demonstrated by the established prognostic signature, known as the angiogenesis-related prognostic risk score (APRS), with regard to prognosis and response to immune checkpoint inhibitor (ICI) therapy.

2. MATERIALS AND METHODS

2.1. Overall Flow Diagram. The flowchart is shown in Figure 1. First, the angiogenesis-related genes with prognostic significance and the differentially expressed genes (DEGs) between normal tissues and UCEC tissues were screened out. The angiogenic subtypes of UCEC patients were constructed by non-negative matrix factorization (NMF) consensus clustering based on the expression profiles of these genes. Then, the multidimensional heterogeneity of angiogenic subtypes was discussed. In addition, APRS was screened by combining Weighted Gene Co-expression Network Analysis (WGCNA) and the least absolute shrinkage selection operator (LASSO) Cox algorithm. The effectiveness of APRS was evaluated in multiple aspects as well.

2.2. Data Sources of Angiogenesis. Genotype-tissue expression (GTEx; https://gtexport.org/home/) and The Cancer Genome Atlas (TCGA; https://portal.gdc.cancer.gov/) databases provided the RNA sequencing (RNA-seq) data and clinical details of UCEC patients. The RNA-seq data of 1550 angiogenesis-related genes were extracted from AMIGO

https://doi.org/10.1021/acsomega.4c03034
ACS Omega 2024, 9, 26519−26539

(https://amigo.geneontology.org/amigo). The criteria for exclusion included the absence of survival data, an overall survival (OS) of less than 30 days, or an unambiguous histological diagnosis. All RNA-seq data were downloaded in the format of fragments per kilobase of exon model per million mapped reads (FPKM) normalized. Table 1 displays the clinicopathological characteristics of UCEC patients in the TCGA.

Table 1. Demographics and Clinicopathological Features of UCEC Patients in TCGA Cohorts

characteristic		number
age	<60	155
	>60	351
stage	Stage I	59
	Stage II	25
	Stage III	74
	Stage IV	17
	unknown	331
histology	endometrioid	307
	mixed	12
	serous	53
	unknown	134
tumor grade	Grade 1	89
	Grade 2	106
	Grade 3	178
	unknown	133
histology grade	EndoGr1	89
	EndoGr2	106
	EndoGr3	112
	MixedGr3	13
	SerousGr3	53
	unknown	133
vital status	alive	418
	dead	88
BMI	<18	1
	18−24	49
	>24	312
	unknown	144
MSI status	MSI-H	127
	MSI-L	20
	MSS	233
	unknown	126
integrative cluster	CN high	60
	CN low	90
	MSI	65
	POLE	17
	unknown	274
PTEN	wild	176
	mutant	325
	unknown	5
TP53	wild	316
	mutant	185
	unknown	5

2.3. Identification of Angiogenesis Subtypes in UCEC Patients. For the purpose of comparing the differential expression of these angiogenesis-related genes between UCEC tissues and normal endometrial tissues, the expression data were normalized using the $\log_2$ (FPKM + 1) transformation. Univariate Cox regression analysis was performed on the 1550 angiogenesis-related genes to determine prognostic angiogenesis-related genes ($P < 0.05$). Then, prognostic angiogenesis-related DEGs were obtained by the intersection between prognostic angiogenesis-related genes with these differentially expressed UCEC-related genes. The "cluster Profiler" package of R was performed to carry out the Kyoto Encyclopedia of Genes and Genomes (KEGG) and Gene Ontology (GO) pathway analysis for functional annotation. The R package "NMF" was used to conduct NMF consensus clustering based on the expression profile of prognostic angiogenesis-related DEGs in order to determine the angiogenesis subtypes of patients. Cophenetic, dispersion, and silhouette indicators assisted in discovering the optimal number of clusters. Through visual inspection, the t-distributed stochastic neighbor embedding (tSNE) approach was utilized to verify the accuracy of the clustering results. The Kaplan−Meier (K−M) survival curve was employed to examine the variations in survival among distinct angiogenesis subtypes. By applying single-sample Gene Set Enrichment Analysis (ssGSEA), the enrichment levels of 50 hallmarks representing varied angiogenesis subtypes that were extracted from the Molecular Signatures Database (MSigDB) were measured.

2.4. Analysis of Genomic Mutations. The somatic mutation spectrum classified by mutation annotation format (MAF) was obtained from TCGA database. Leveraging the R software package "Maftools", we analyzed and visualized the mutation spectrum and frequencies of genes in different angiogenic subtypes. Mutations per megabase (mut/Mb) were calculated to compute the tumor mutation burden (TMB).[12] Meanwhile, TCGA database contained copy number alteration (CNA) data of UCEC patients, and GISTIC2.0 was utilized to detect substantial whole genome amplifications or deletions.[13] The total number of genes corresponding to CNA burden with copy number changes at the focal and arm levels.[14]

2.5. Evaluation of TIME and Immunotherapy Responses. The immune score, matrix score, estimated score, and tumor purity of UCEC patients were determined using the R software package "estimate".[15] The enrichment scores of 29 immune signals were calculated by ssGSEA.[16] According to the Z-score of the ssGSEA for the 29 immune signals mentioned above, patients were grouped into subtypes with high-/low-immunity. The CIBERSORT algorithm with 1000 permutations was executed to estimate the fractions of immune cells infiltrating 22 tumors.[17] The tumor immune dysfunction and exclusion (TIDE) algorithm was implemented to assess the possible response of ICI treatment and can be available at http://tide.dfci.harvard.edu. More likely, patients with lower TIDE scores or higher microsatellite instability (MSI) scores exhibited stronger responses to the ICI treatment.

2.6. Construction of an Angiogenesis-Related Prognostic Signature. WGCNA was carried out using the R software package "WGCNA" to identify hub genes associated with angiogenic subtypes on the expression profile of prognostic angiogenesis-related DEGs.[18,19] To ascertain the appropriate soft-thresholding power, the conventional scale-free model fitting index R2 was adopted. And then, the correlation between modules and angiogenic subtypes was examined by the computation of module characteristic genes. The hub genes that were most closely related to the angiogenic subtypes in the module were discovered. In order to construct an angiogenesis-related prognostic signature, hub genes were incorporated in the LASSO Cox regression. The APRS was calculated as follows:

https://doi.org/10.1021/acsomega.4c03034
ACS Omega 2024, 9, 26519−26539

$$\mathrm{APRS} = \sum_{i=1}^{n} coefi^{*}xi$$

Among them, *xi* refers to the expression level of selected hub genes, while *Coe fi* is the corresponding LASSO coefficient. K−M survival analysis was performed to compare overall survival (OS) and progression-free survival (PFS) among the angiogenic subtypes in order to evaluate the prognostic significance of APRS. Univariate and multivariate Cox regression analyses were carried out to determine the independent prognostic value of APRS. To investigate the effect of angiogenesis on the progression of UCEC, we elucidated the relationship between angiogenesis and clinicopathological factors, including age, stage, pathological grade, molecular classification, survival status, and risk score. In addition, we exploited a random-effects meta-analysis approach to determine the APRS's pooled hazard ratio (HR).

2.7. Establishment of Predictive Nomogram. Multivariate Cox regression analysis was incorporated using clinical variables to examine the prognostic significance of the angiogenesis fraction. The prognostic nomogram of TCGA data set for predicting 1-year, 3-year, and 5-year OS in UCEC patients was constructed.[20] The calibration curve was applied to assess the consistency between the predicted survival and the actual survival period. The receiver operating characteristic (ROC) curves over time were utilized to estimate the specificity and sensitivity of the model.

2.8. Tissue Samples Collection. UCEC and paratumor tissues in total were taken from patients undergoing surgery in the obstetrics and gynecology department at Union Hospital, Tongji Medical College, Wuhan, China. Table S1 provides a summary of the clinical data. The Institutional Review Board of Tongji Medical College of Huazhong University of Science and Technology approved all the research programs (IRB approval number: [2021]-S046).

2.9. Cell Culture and Transfection. Human endometrial cancer cell lines (RL-952, KLE, HEC-1B, HEC-1A, and Ishikawa), normal human endometrial epithelial cells (hEECs), and human umbilical vein endothelial cells (HUVECs) were purchased from the American Type Culture Collection (ATCC). The cell lines were characterized by Zhong Qiao Xin Zhou Biotechnology Corporation using short tandem repeat (STR) markers. RL95-2, KLE, Ishikawa, HEC-1-B cells, and hEECs were cultured in DMEM/F12 medium, HEC-1 A cells were maintained in McCoy's 5 A medium (Gibco) supplemented with 10% fetal bovine serum (FBS)(Gibco) and 1% streptomycin and penicillin (Bosterbio) in a 37 °C, 5% CO_2 incubator.

In order to construct IHH, TUBG1, and EEF2 overexpression plasmids, human IHH, TUBG1, and EEF2 and their complementary DNA (cDNA) were synthesized by Genomeditech (Shanghai, China) and cloned into the PGMLV-CMV-MCS-3 × Flag-EF1-ZsGreen1-T2A-Puro vector. MECP2 short hairpin RNA (shRNA) was synthesized by Genomeditech (Shanghai, China) and cloned into the PGMLV-hU6-MCS-CMV-Puro vector. The shRNA sequences used are shown in Table S2. HEC-1B and Ishikawa cells were seeded in six-well plates and transfected with 2 μg of expression plasmid using Lipofectamine 3000 (Invitrogen, CA, USA). Total RNA was isolated 48 h after transfection, and qPCR was performed to verify transfection efficiency. The conditioned medium (CM) was collected, centrifuged, and filtered to culture HUVECs.

2.10. RNA Isolation and Quantitative Real-Time PCR (qRT-PCR). Total RNA was isolated from cells or tissues using TRizol reagents (Takara, Otsu, Japan) and reversely transcribed into cDNA using 4× Hifair III SuperMix plus (Yeasen, Shanghai, China). Real-time PCR analysis was performed using Hieff qPCR SYBR Green Master Mix (Yeasen, Shanghai, China) on a CFX Connect real-time PCR detection system (Bio-Rad, Hercules, CA, USA). GAPDH was selected as the internal reference for the standardization of qPCR results, and the expression level of RNA was calculated by the $2^{-\Delta\Delta CT}$ method. All primers used are listed in Table S2.

2.11. Wound-Healing and Transwell Assays. Endothelial cell migration is one of the hallmarks of angiogenesis and serving as a pivotal initial stage in the angiogenic process.[21−24] Wound-healing assay is a fundamental technique utilized to evaluate cell migration ability. Endothelial cells are cultured to confluence within a dish and then scraped with a pipet tip, allowing the endothelial cells at the wound edge to migrate into the scraped area.[25] HUVECs were incubated with the above CM in six-well plates and cultured until 90% confluence. A constant diameter strip was created using 200 μL pipet tip across the center of the well, and detached cells were removed by washing with phosphate buffer saline (PBS). Photographs were taken at 0 and 24 h after serum-free medium was added to a six-well plate. Quantitative analysis was performed by ImageJ software (Bethesda).

Transwell assay describes the migration ability of tumor cells to chemokines through the vascular endothelium. Endothelial cells are placed in the upper compartment and allowed to migrate through the pores of the membrane to the lower compartment. Objective Chemokines or chemokines of secretory cells exist in the lower compartment.[26] HUVECs incubated with serum-free medium were seeded in the top chamber of 8 mm pore size 24-well plates (Corning, USA) at a density of 1×10^4 cells/0.2 mL. Then, 0.6 mL of transfected Ishikawa cells or HEC-1B cell suspension was added in the lower chamber. After 24 h, cells that did not migrate through the pores on the surface of the membrane were wiped with a cotton swab. while cells migrated through the pores were fixed with 4% paraformaldehyde for 10 min, stained with 0.1% crystal violet, and photographed with a 10X microscope (Olympus, JPN).

2.12. Tube Formation Assay. Endothelial tube formation assay is one of the most extensive and reliable methods to study in vitro angiogenesis. Endothelial cells are inoculated on the basement membrane extract and subjected to angiogenic factors in the conditioned medium to form a rapid and quantifiable tube network within hours.[27] Briefly, Matrigel (Corning, USA) and DMEM-F12 were mixed in a 1:1 ratio. A total of 50 μL of Matrigel-DMEM-F12 matrix was added to each well of the 48-well plate. HUVECs (1×10^5) resuspended in the CM and CM control were seeded in a Matrigel-coated well in triplicate and incubated at 37 °C for 4 h. Five pictures per well (center of the well and four cardinal points) were taken by using an inverted phase contrast microscope (Nikon, Japan). For statistical analyses, three wells were seeded per conditions. ImageJ with the Angiogenesis Analyzer plugin was applied to measure the total tubular length and number of tubules to evaluate angiogenesis.

2.13. Immunohistochemistry (IHC). Paraffin-embedded clinical tissue specimens and mouse tumor tissue sections were dewaxed, dehydrated, rehydrated, and repaired with citric acid. Subsequently, the tissue sections were incubated with primary antibodies after peroxidase blocking at 4 °C overnight. The

https://doi.org/10.1021/acsomega.4c03034
ACS Omega 2024, 9, 26519−26539

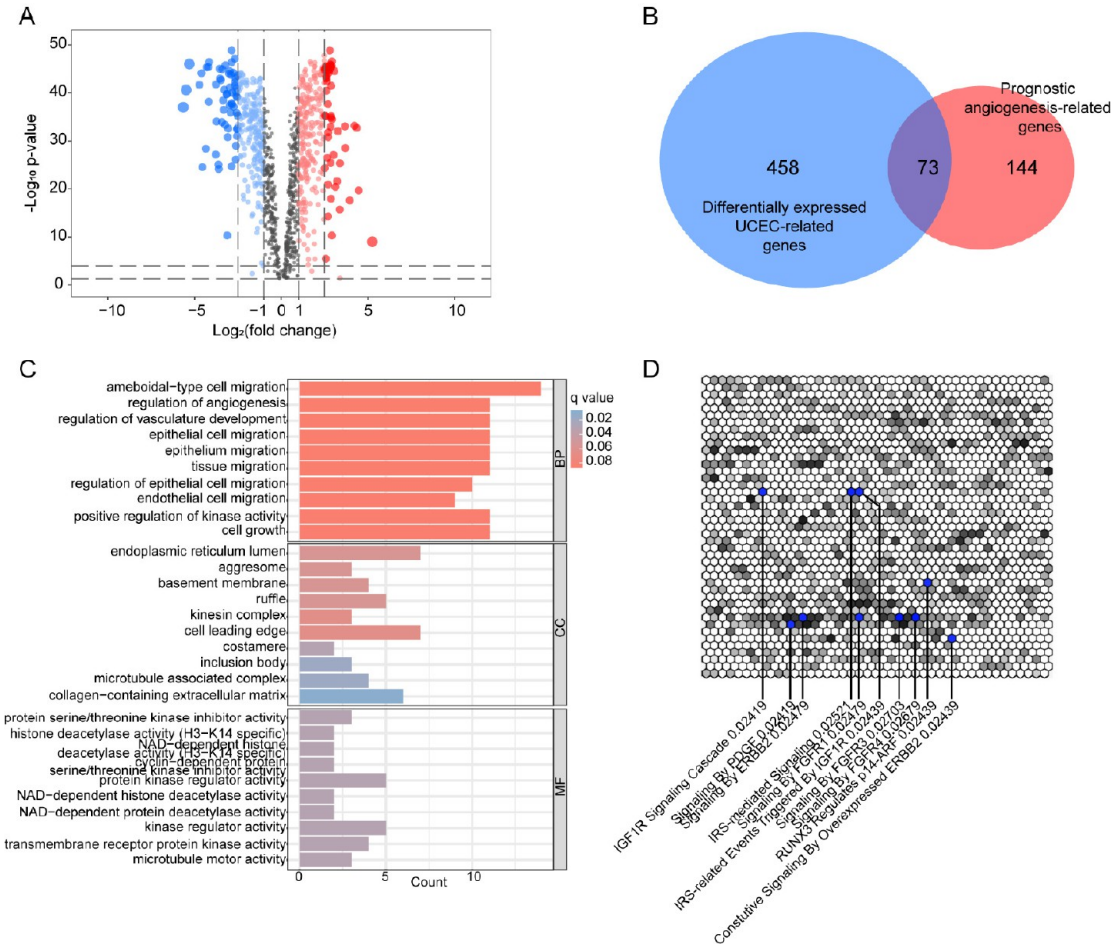

Figure 2. Identification of prognostic angiogenesis-related DEGs of UCEC. (A) Volcano plot of DEGs ($P < 0.05$ and $|\log_2 FC| > 1.5$) between UCEC tissues and normal tissues in TCGA cohort and GTEx database. (B) Venn diagram identified 73 prognostic angiogenesis-related DEGs. (C,D) GO terms and hexagonal canvas plot significantly enriched in prognostic angiogenesis-related DEGs.

secondary antibodies were incubated at 37 °C for 1 h and then washed with PBS. The sections were restained with hematoxylin and detected with a light microscope after adding diaminobenzidine. Antibodies can be found in Table S3.

2.14. Tumor Xenograft Model. The animal studies were approved by the Institutional Animal Care and Use Committee of Huazhong University of Science and Technology (ethical approval number: [2023]-3357). BALB/c 5-wk-old female nude mice were purchased from Vital River (Beijing, China) maintained in a standard pathogen-free environment laboratory. Five mice in each group were injected subcutaneously with IHH, TUBG1, and EEF2 overexpression, shMECP2 or control cells bilaterally. The subcutaneous tumor size was measured weekly until the mice were sacrificed by cervical dislocation on the 28th day after cell implantation, and the tumors were removed and weighed. The expression of CD31 and K_i-67 in xenograft tumors was determined by IHC.

2.15. Single-Cell Sequencing Data Analysis. The single-cell sequencing data SRP3349751[28] containing five normal endometrial tissues, five endometrioid endometrial cancer (EEC) primary tissues, and five atypical endometrial hyperplasia (AEH) tissues was downloaded from the NCBI SRA database. The expression matrix was preprocessed using the 'Seurat' R package to remove low-quality cells, and the data was integrated and normalized by the 'NormalizeData' package. After employing the "runPCA" to perform principal component analysis (PCA), cells were alternately clustered at the highest resolution by 'FindClusters'. The *t*-distributed stochastic neighborhood embedding method (tSNE) was utilized to visualize the data.

2.16. Statistical Analysis. R software (version 4.2.0) and GraphPad Prism (version 7) were applied to all statistical analysis and graphical visualization. Student *t* test or Wilcoxon sign rank test was used for comparison between two groups and one-way ANOVA for comparisons among more than two groups. To evaluate the differences in overall survival among the subgroups, the log-rank test was executed. Spearman correlation analysis was employed to assess the correlation between the two parameters. $P < 0.05$ was considered statistically significant.

3. RESULTS

3.1. Angiogenesis-Related Genes. Transcriptome data of 531 differentially expressed UCEC-related genes were obtained from TCGA cohort and GTEx database (Table S4), of which 270 were up-regulated and 261 were down-regulated in UCEC (Figure 2A). A total of 1550 angiogenesis-related genes (Table S5) were obtained from AMIGO. We then explored the intersection between 217 prognostic angiogenesis-related genes (Table S6) acquired by univariate Cox regression analysis with these DEGs. Finally, 73 prognostic angiogenesis-related DEGs were identified (Figure 2B and Table S7). The top significantly enriched GO terms and hexagonal canvas plot for these

https://doi.org/10.1021/acsomega.4c03034
ACS Omega 2024, 9, 26519−26539

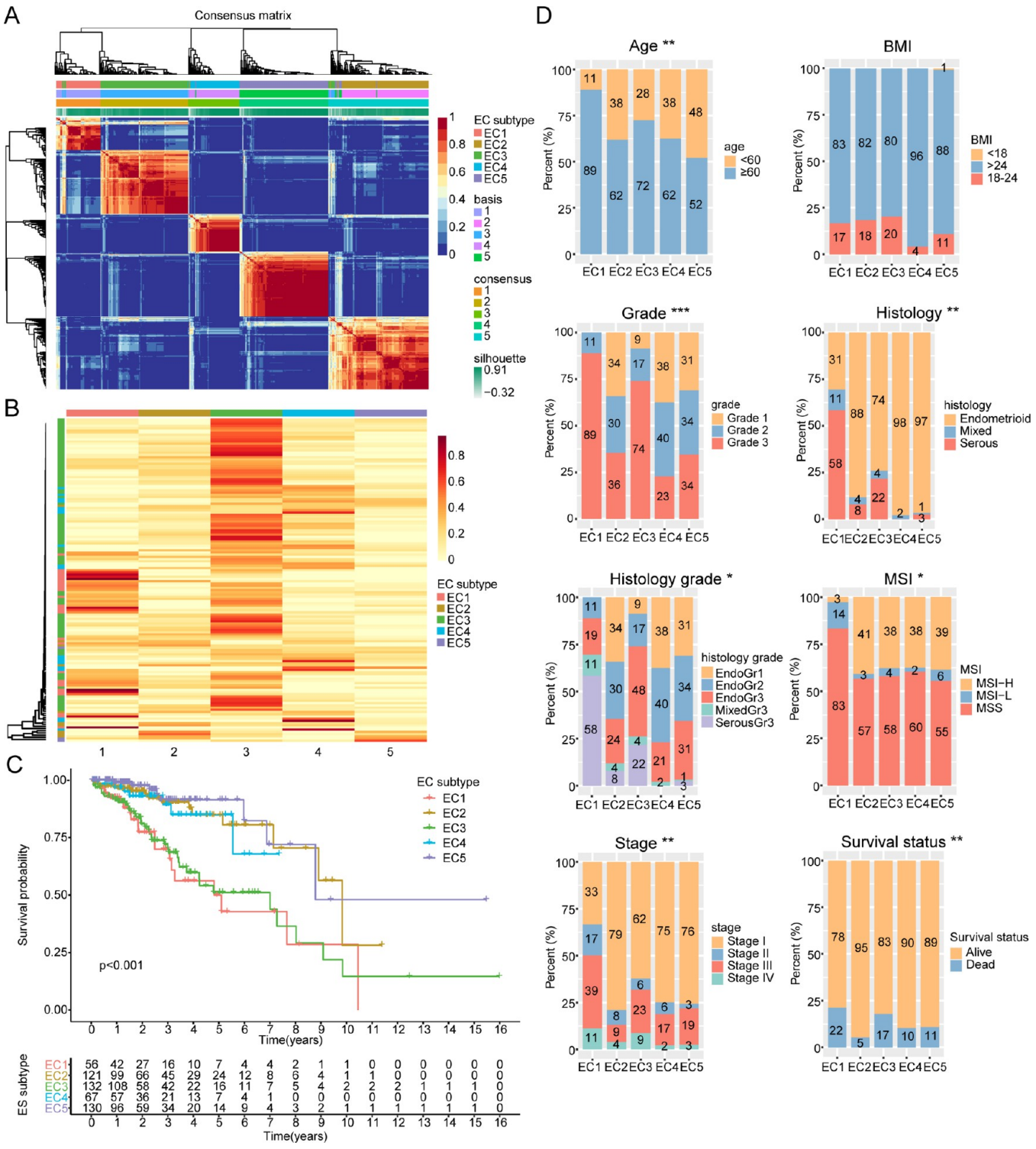

Figure 3. Identification and comparisons of the angiogenesis subtypes of UCEC. (A) Consensus map of NMF clustering. (B) Heatmap demonstrated the expression levels of 73 prognostic angiogenesis-related DEGs among angiogenesis subtypes. (C) Kaplan−Meier survival analysis exhibited significantly different OS among angiogenic subtypes. (D) Comparisons of age, BMI, WHO grade, histology, histology grade, MSI, stage, and survival status among angiogenic subtypes. *$P < 0.05$, **$P < 0.01$, and ***$P < 0.001$.

prognostic angiogenesis-related DEGs are presented in Figure 2C,D.

3.2. Identification of Angiogenesis Subtypes in TCGA Cohort. NMF was performed to identify angiogenesis subtypes in TCGA cohort based on 73 prognostic angiogenesis-related DEGs. Five was selected as the optimal number of clusters, which was determined by cophenetic, dispersion, and silhouette indicators (Figure S1A). Then, five subgroups, including 506 UCEC patients, were identified (Figure 3A), namely EC1 (n = 56), EC2 (n = 121), EC3 (n = 132), EC4 (n = 67), and EC5 (n = 130). The tSNE revealed notable variations in the distribution of the five angiogenic subtypes (Figure S1B). The heat map

https://doi.org/10.1021/acsomega.4c03034
ACS Omega 2024, 9, 26519−26539

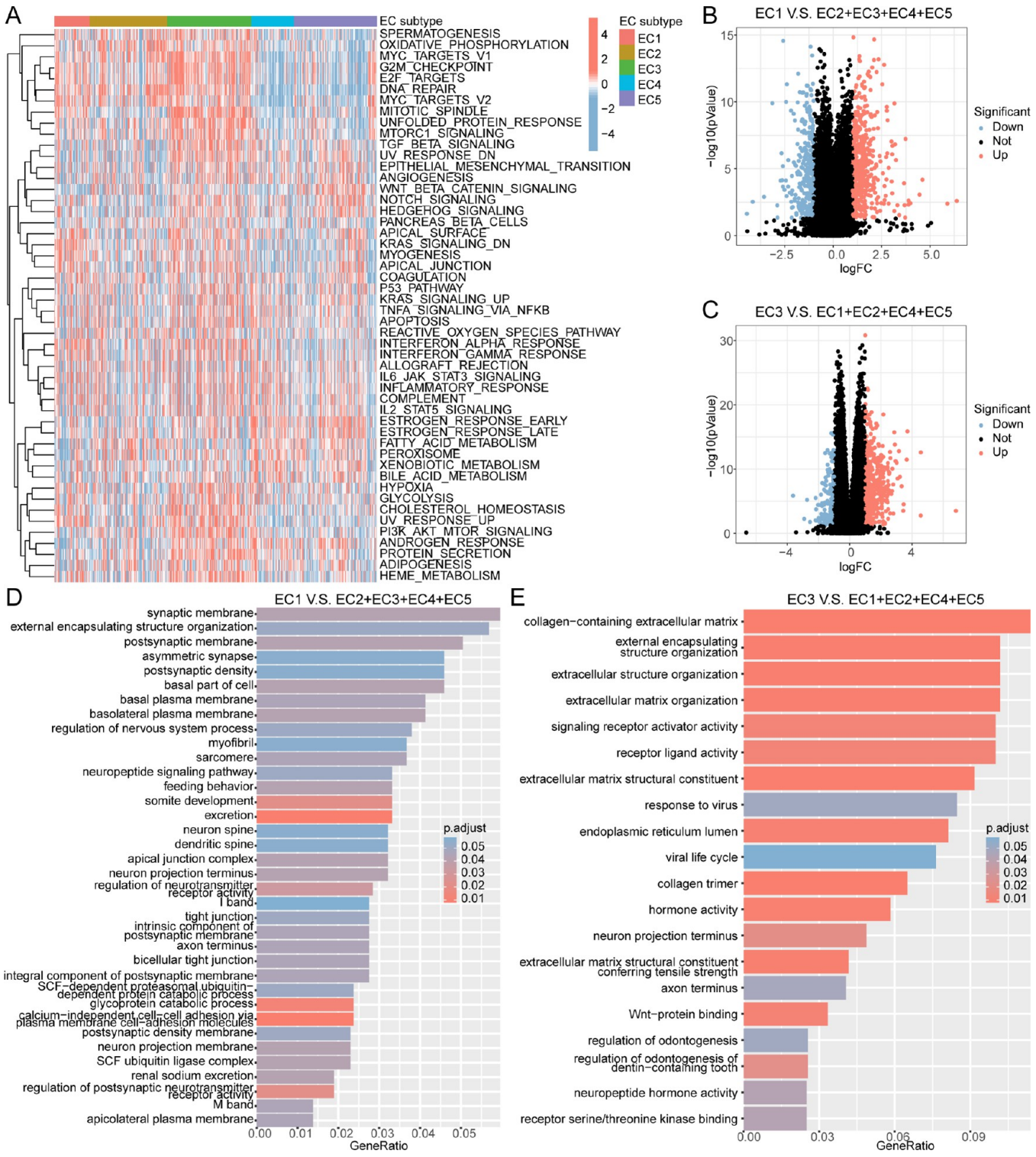

Figure 4. Comparisons of cancer hallmarks among angiogenic subtypes. (A) Heatmap illustrated the ssGSEA *Z*-scores of 50 hallmarks among angiogenic subtypes. Red represented high scores, and blue represented low scores. (B, C) Volcano plots showed DEGs ($P < 0.05$ and |log2FC| > 1) in EC1 and EC3 subgroups. (D, E) Gene Ontology enrichment analysis for significantly upregulated genes in EC1 and EC3, respectively.

revealed enormous differences in the expression of 73 prognostic angiogenesis-related DEGs (Figure 3B). The K−M survival curve displayed a demonstrable survival difference among the five angiogenic subtypes (Figure 3C). EC5 had the best survival outcome, while EC1 and EC3 had the poorest.

We then compared the demographic and clinicopathological characteristics of UCEC patients with five angiogenic subtypes. Figure 3D shows that, compared with other subtypes, EC1 and EC3 had more patients older than or equal to 60 years old. There were no obvious differences among subtypes in terms of the BMI distribution. Significant differences in pathological grade and clinical stage among the five subtypes were observed. EC1 and EC3 possessed a noticeably greater percentage of World Health Organization (WHO) grade III UCEC and serous UCEC

https://doi.org/10.1021/acsomega.4c03034
ACS Omega 2024, 9, 26519−26539

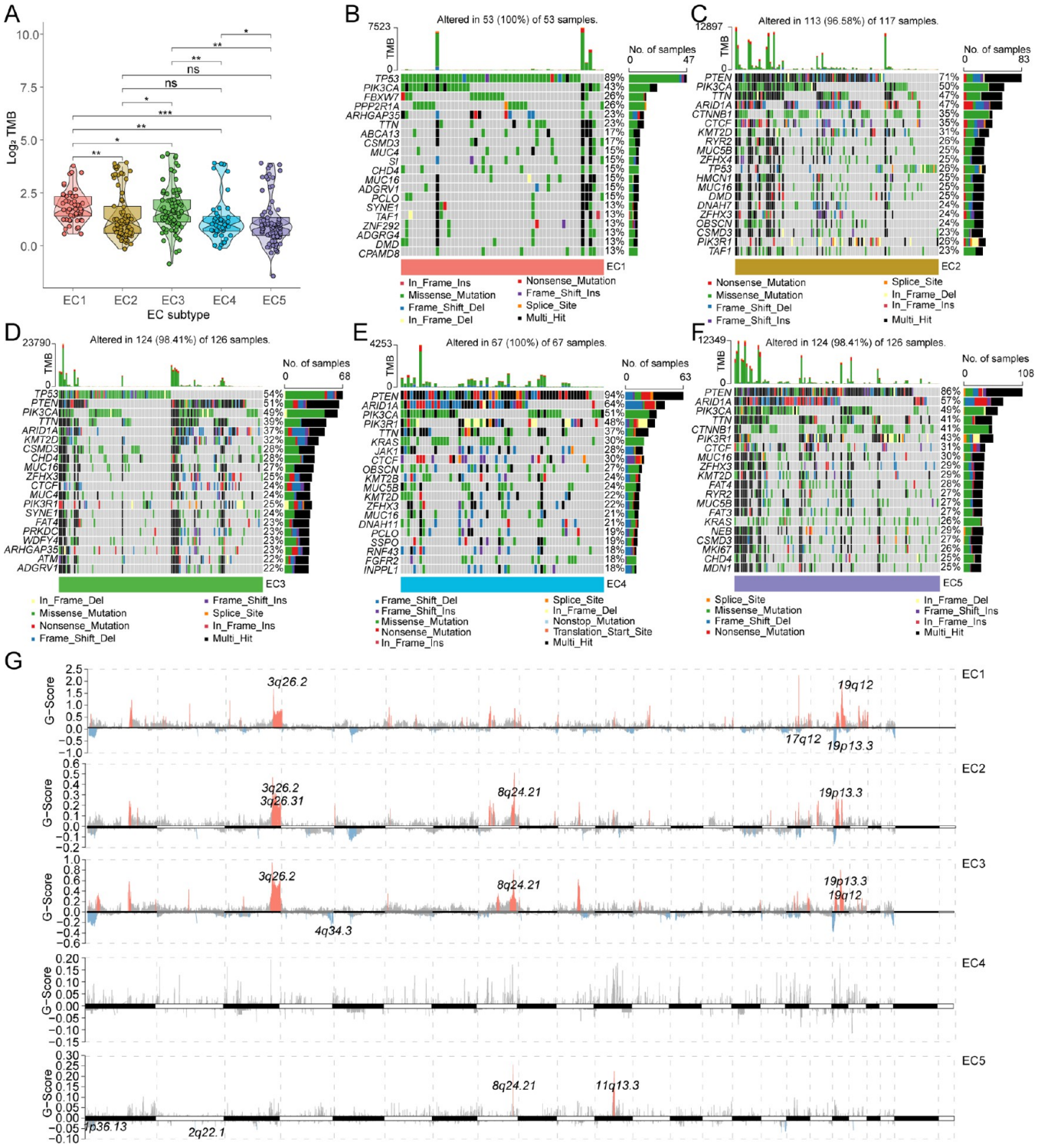

Figure 5. Comprehensive analyses of genomic mutations among angiogenic subtypes. (A) Comparisons of TMB among angiogenic subtypes. (B−F) Mutation profiles of angiogenic subtypes. (G) Gistic score distribution of all autosomes in angiogenic subtype. * $P < 0.05$, ** $P < 0.01$, *** $P < 0.001$, and ns No significance.

compared with EC2, EC4, and EC5. Simultaneously, EC1 and EC3 had the lowest proportion of MSI-H and the highest proportion of clinical stages III and IV. Of note, a higher mortality rate was investigated in EC1 and EC3.

In order to explore the potential molecular mechanisms associated with UCEC angiogenesis subtypes, ssGSEA was performed using transcriptome data from 50 gene sets obtained from MSigDB. We used the ssGSEA *Z*-score to measure the level of the 50 hallmarks and visualized them through a heat map (Figure 4A). Compared with EC2, EC4, and EC5, EC1 and EC3 were more involved in these hallmarks correlated with cell cycle and DNA repair, particularly EC3, which may portend active proliferation of cancer cells. Beyond that, EC1 showed a positive correlation with cell junctions and ECM. EC3 was positively correlated with numerous cancer-related hallmarks, including metabolism, apoptosis, epithelial-mesenchymal transition

https://doi.org/10.1021/acsomega.4c03034
ACS Omega 2024, 9, 26519−26539

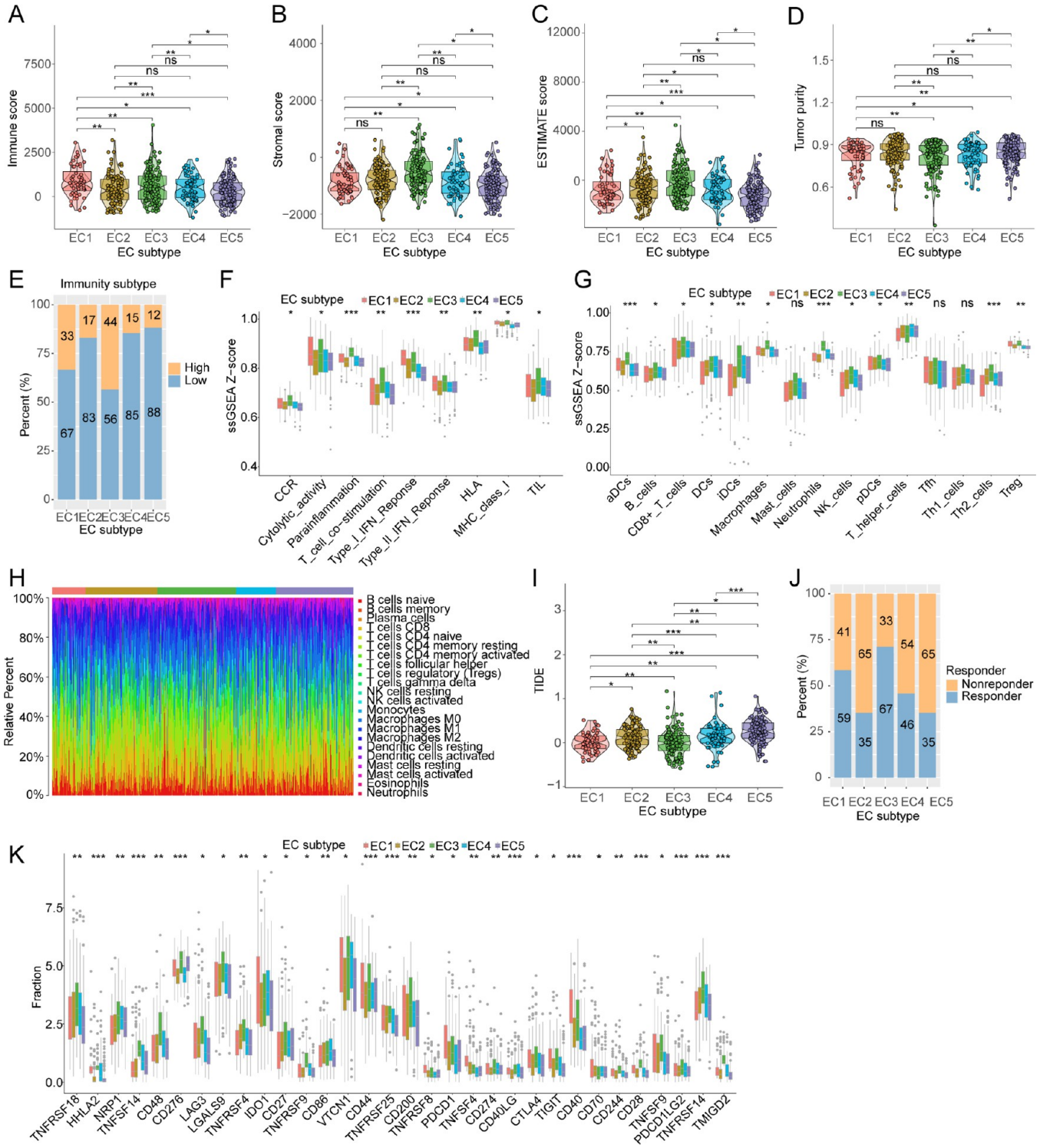

Figure 6. Different TIME patterns and immunotherapeutic responses of angiogenic subtypes. (A−D) Comparison of immune scores, stromal scores, ESTIMATE scores, and tumor purity among angiogenic subtypes. (E) Different proportion of high- and low-immunity tumors among angiogenic subtypes. (F,G) Levels of immune cell infiltrations and immune functions quantified by the ssGSEA Z-score among angiogenic subtypes. (H) Proportion of 22 immune cells quantified by the CIBERSORT algorithm among angiogenic subtypes. (I) Comparison of TIDE scores among angiogenic subtypes. (J) Proportion of ICI therapy responders predicted by the TIDE algorithm among angiogenic subtypes. (K) Comparison of immune checkpoint expressions among angiogenic subtypes. * $P < 0.05$, ** $P < 0.01$, *** $P < 0.001$, and ns No significance.

(EMT), and inflammation. To gain further insights, we in the aggregate screened out 475 upregulated genes ($\log_2$FC > 1 and $P < 0.05$), 285 downregulated genes ($\log_2$FC<−1 and $P < 0.05$) in EC1, 513 upregulated genes ($\log_2$FC > 1 and $P < 0.05$), and 151 downregulated genes ($\log_2$FC<−1 and $P < 0.05$) in EC3 (Figure 4B,C). The enrichment biological processes of up-regulated genes in EC1 and EC3 were in agreement with the results of ssGSEA (Figure 4D,E). The preceding results may elucidate the poor outcomes of EC1 and EC3 to a certain degree.

https://doi.org/10.1021/acsomega.4c03034
ACS Omega 2024, 9, 26519−26539

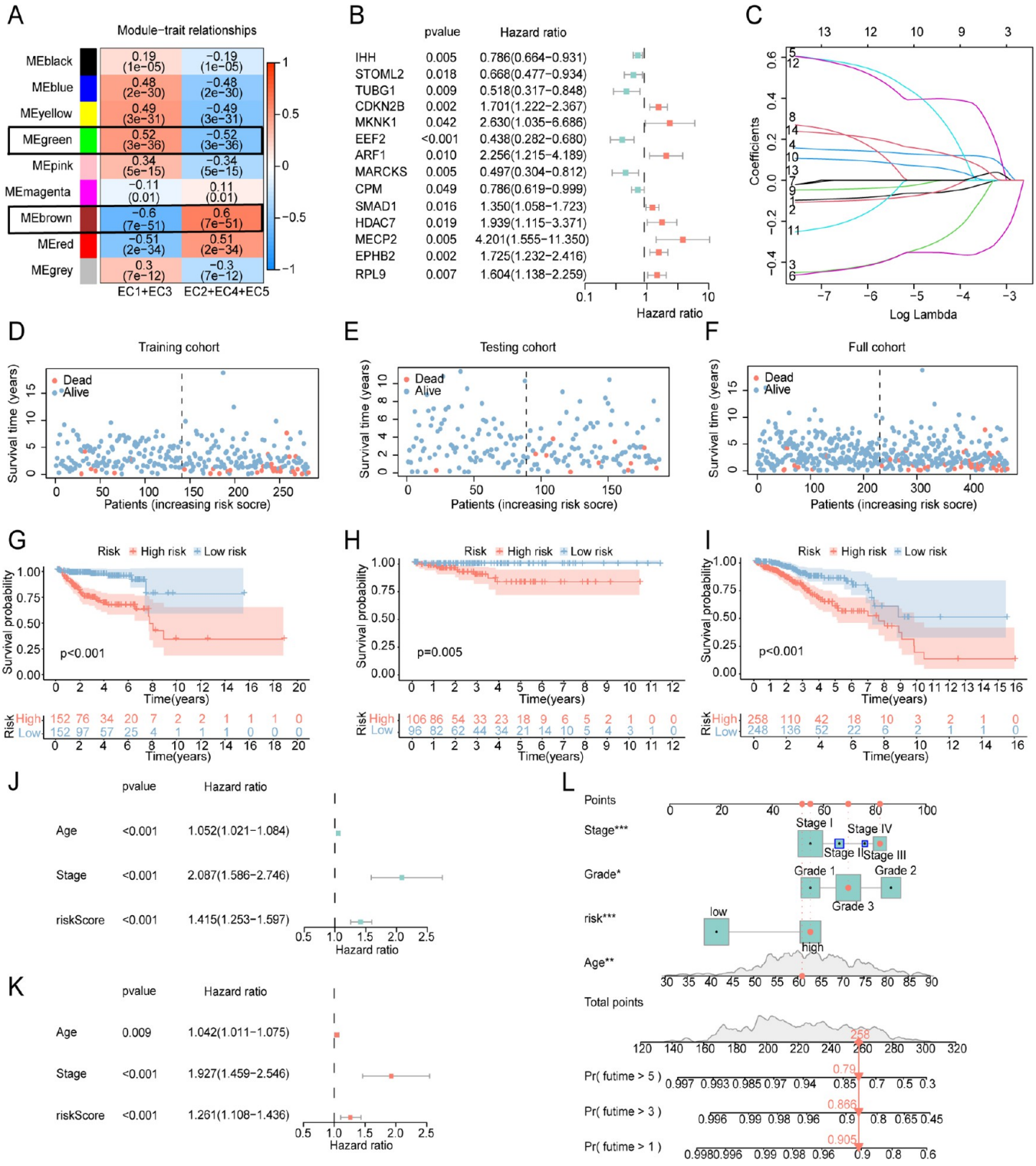

Figure 7. Construction and validation of a prognostic signature based on angiogenesis-related hub genes. (A) Correlations of 9 modules with angiogenic subtypes. The green model and brown model were selected and highlighted with a black box. (B) Univariate Cox regression analysis to screen 14 prognostic angiogenesis-related hub genes. (C) LASSO regression curve of 14 prognostic angiogenesis-related hub genes with minimal lambda value. (D−F) Scatter diagrams showing the survival time of patients based on the risk score in each cohort. (G−I) K−M Survival curves of OS according to high-APRS and low-APRS subgroups in patients with UCEC of each cohort. (J,K) Univariate and multivariate Cox regression analysis of age, stage, and risk score for OS. (L) Prognostic nomogram predicts 1-, 3-, and 5-year survival probability of UCEC patients.

3.3. Comprehensive Analysis of Genomic Mutations among Angiogenic Subtypes. To shed more light on the discrepancy in genomic layers, we contrasted the somatic mutation spectrum and CNA landscape among angiogenic subtypes. First, the TMB of EC1 and EC3 was significantly higher than that of EC2, EC4, and EC5 (Figure 5A). The somatic mutation spectrum indicated that EC1 and EC3 displayed specific top mutation genes, in contrast to the other

https://doi.org/10.1021/acsomega.4c03034
ACS Omega 2024, 9, 26519−26539

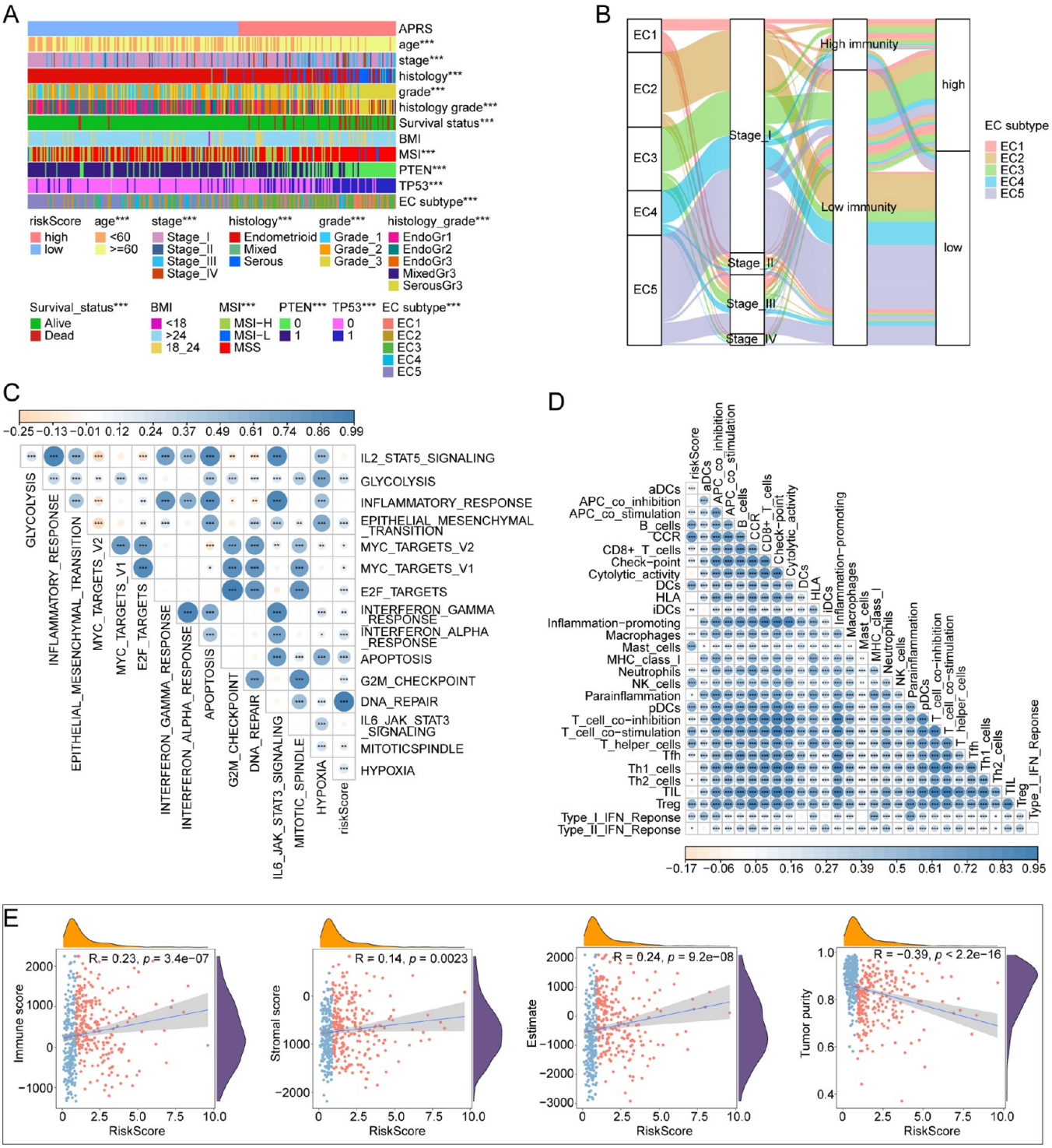

Figure 8. Correlation of APRS with clinicopathological features, genomic mutations, and TIME patterns in TCGA cohort. (A) Overview of the correspondence between APRS and other features of UCEC patients. (B) Sankey diagram showed the attribute changes of the EC subtype, FIGO stage, immune subtype, and APRS. (C) Correlation between APRS and well-known cancer hallmarks. (D) Correlation between APRS and the ssGSEA Z-scores of 29 immune signatures. (E) Correlation of APRS with immune scores, stromal scores, ESTIMATE scores, and tumor purity. * $P < 0.05$, ** $P < 0.01$, *** $P < 0.001$, and ****$P < 0.0001$.

three angiogenesis subtypes. TP53 was the most frequently altered gene in EC1 and EC3. Nevertheless, PTEN was the most common mutant gene in EC2, EC4, and EC5 (Figure 5B−F). Figure 5G depicts the copy number distribution of angiogenic subtypes as well as gains and losses in gene copy numbers, which were arranged according to the chromosomal location, extending from chromosomes 1−22. Taken together, the data above demonstrated the active genomic mutations in EC1 and EC3, which may be attributed to their stronger proliferation capacity of cancer cells.

3.4. TIME and Immunotherapeutic Responses in Different Angiogenic Subtypes. Angiogenesis may play an

https://doi.org/10.1021/acsomega.4c03034
ACS Omega 2024, 9, 26519−26539

essential part in regulating TIME, as more and more research has shown, and targeting angiogenesis could be a meaningful regulatory strategy for immunotherapy.[29−32] Accordingly, we made an effort to contrast the immunotherapeutic responses and TIME patterns among various angiogenic subtypes. The ESTIMATE algorithm was carried out to quantify the components of the TIME of UCEC. The results suggested that EC1 and EC3 possessed lower tumor purity as well as higher immune, stromal, and ESTIMATE scores compared to the other three subtypes. Opposite trends were observed in EC2, EC4, and EC5 (Figure 6A−D). Then, according to the ssGSEA Z-score of 24 immune signatures, we classified UCEC patients into high-/low-immunity subtypes. EC1 and EC3 incorporated a higher proportion of high-immunity subtypes, whereas EC2, EC4, and EC5 mainly consisted of low-immunity subtypes ($P < 0.001$; Figure 6E). The distribution of ssGSEA *Z*-scores of 9 immune functions and 15 immune cell infiltrations is presented in Figure 6F,G. First and foremost, EC1 and EC3 exhibited a higher proportion of immune cell infiltration and more powerful immune function than the other three subtypes. CIBERSORT, an additional method, was also applied to describe the proportion of 22 immune cells in different angiogenesis subtypes, as shown in Figure 6H.

ICI therapy has undoubtedly been a prospective immunotherapy approach up to this point, which has led to an enormous improvement in antitumor therapy. Therefore, we additionally utilized the TIDE algorithm to forecast how different angiogenesis subtypes would react with ICI treatment. It revealed that the TIDE scores of EC1 and EC3 were decreased markedly (Figure 6I). The proportion of responders in EC1 and EC3 subtypes was almost twice as high as that in EC2 and EC5 subtypes ($P < 0.001$; Figure 6J). EC1 and EC3 may be stronger candidates for ICI therapy. In the bargain, we evaluated immune checkpoint expression levels among angiogenic subtypes, including CD276, LAG3, LGALS6, LAG-3, TNFRSF9, VTCN1, CD44, CD200, TNFRSF8, PDCD1, CD274, CTLA4, TIGIT, CD40, CD70, CD244, CD28, and TNFSF9 (Figure 6K). All of this evidence pointed to a potential critical function for the angiogenesis pattern of UCEC patients to influence TIME patterns and immune treatment responses.

3.5. Establishment and Validation of a Prognostic Signature Based on Angiogenesis-Related Hub Genes. Using the transcriptome data of 73 prognostic angiogenesis-associated DEGs, WGCNA analysis was performed to recognize hub genes relevant to angiogenesis. On the basis of the conventional scale-free model fitting index R2, 4 was selected as the optimal soft-thresholding power (Figure S2A). Then, we obtained a total of 9 gene modules (Figure 7A). In view of previous findings, similarities existed in survival, genomic mutations, and immune characteristics between EC1 and EC3, as well as between EC2, EC4, and EC5. Hence, EC1 and EC3, and likewise EC2, EC4, and EC5, were merged together (Figure 7A, Figure S2B). Among these 9 models, the brown module, comprising 17 genes, declared to have the strongest association with EC1 and EC3, while the green module containing 13 genes demonstrated the highest correlation with EC2, EC4, and EC5 (Figure 7A). Whereupon 30 genes in the two models were defined as hub genes related to angiogenesis and selected for further analysis. Figure S2C,D exhibits the enriched GO terms and KEGG pathways of the green and brown module genes.

Furthermore, we integrated these 30 angiogenesis-related hub genes into the LASSO Cox regression in TCGA cohort, and 14 representative genes were identified in the establishment of a prognostic signature related to angiogenesis (Figure 7B,C). Six protective genes, which were IHH, STOML2, TUBG1, EEF2, MARCKS, and CPM, and eight risky genes, including CDKN2B, MKNK1, ARF1, SMAD1, HDAC7, MECP2, EPHB2, and RPL9, had an impact on survival outcomes (Figure 7B). Figure 7C reveals the LASSO regression curve of each selected gene in the signature.

To establish a credible prognostic signature for UCEC patients, 506 patients were divided into a training cohort and a testing cohort according to a ratio of 3:2. The expression level of each selected angiogenesis-related hub gene and the associated LASSO coefficients were multiplied to determine the APRS values for each UCEC patient. High-APRS and low-APRS subgroups of patients were distinguished based on the optimal cutoff value (as shown in Figure S2E). A scatter diagram displaying the patient's survival time was also created based on the risk score. As the risk score increased, the number of deaths increased, and the survival time of patients gradually decreased (Figure 7D−F). As proven in the K-M survival curve, worse OS was present in patients with high-APRS subgroups in TCGA cohort (Figure 7I). It identically showed a high degree of consistency in the training cohort and testing cohort (Figure 7G,H), which indicated that the increased risk of angiogenesis reflected the poor prognosis of UCEC patients. The heat map revealed that the four representative genes, MECP2, TUBG1, IHH, and EEF2, were differentially expressed in the high-APRS group and the low-APRS group in each cohort (Figure S2F), and the K-M curves of the above four representative genes are shown in Figure S3A. According to univariate Cox regression analysis, APRS was an independent predictor of poor OS in UCEC patients (HR = 1.415,95% CI: 1.253−1.597), as well as the multivariate Cox regression analysis (Figure 7J,K). In addition, a nomogram combining APRS and other clinicopathological features involved in age, stage, and grade was performed to evaluate 1-, 3-, and 5-year survival for predicting the probability of clinical outcomes. The results revealed that the OS of UCEC patients declined in pace over time (Figure 7L). Therefore, APRS could be applied as an efficacious prognostic marker for UCEC patients.

3.6. Correlation of APRS with Clinicopathological Features, Genomic Mutations, and TIME Patterns. Since the prognostic value of APRS had been well elucidated, we attempted to explore its clinical relevance in TCGA cohort. Figure 8A arranged APRS from low to high to demonstrate its correlation with clinical pathological features. Dramatic differences existed in the high- and low-APRS subgroups in aspects of age, stage, histology, grade, histological grade, survival status, MSI, PTEN mutation, TP53 mutation, and EC subtypes. Strikingly, the BMI distribution still did not show significant differences. The EC subtype, FIGO stage, immune subtype, and APRS of each patient were visualized by the Sankey diagram (Figure 8B). We also compared the APRS levels among subgroups stratified according to different clinicopathological features. Significantly higher levels of APRS were observed in patients with clinicopathological features of age ≥60 years, WHO grade III, FIGO stage III, histological mixed and serous UCEC, mixed grade III and serous grade III, MSS, death, EC1 and EC3 subtypes, TP53 mutation, and PTEN wild, whereas no differences in APRS existed in patients with BMI stratification (Figure S3B).

We examined the correlation between cancer hallmarks and APRS to better describe the prognostic signature related to angiogenesis. A bubble plot revealed that a significant

https://doi.org/10.1021/acsomega.4c03034
ACS Omega 2024, 9, 26519−26539

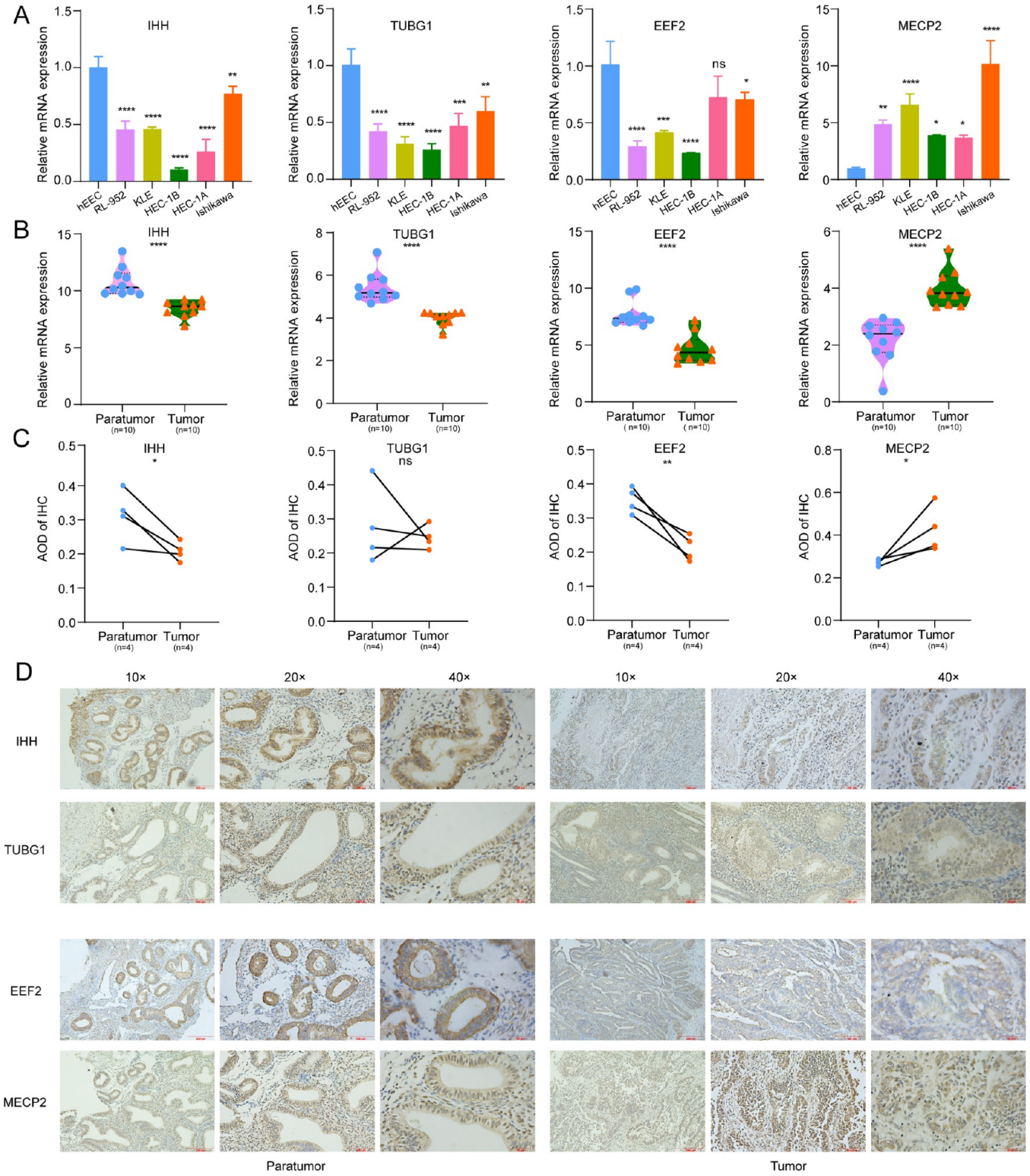

Figure 9. Expression levels of selected angiogenesis-related hub genes. (A) Differential transcription levels of IHH, TUBG1, EEF2, and MECP2 in UCEC cell lines and hEECs. (B) Violin diagrams of differential transcript levels of IHH, TUBG1, EEF2, and MECP2 in UCEC tissues and paratumor tissues. (C) Comparison of the protein expression levels of IHH, TUBG1, EEF2, and MECP2 between UCEC and paratumor by immunohistochemistry staining and analyzed by calculating average optical density (AOD: IOD/area). (D) Representative immunohistochemistry staining images. *P < 0.05, **P < 0.01, ***P < 0.001, ****P < 0.0001, and ns no significance.

correlation between APRS and many storied cancer hallmarks, including inflammation, metabolism, EMT, and cell cycle-related markers, was observed (Figure 8C). In consideration of the association between APRS and different immune subtypes, we took a more particular knowledge of the details and differences in TIME patterns once the APRS changed. The correlation between APRS and 29 immune signatures was also illustrated by a bubble plot in TCGA cohort (Figure 8D). It can

https://doi.org/10.1021/acsomega.4c03034
ACS Omega 2024, 9, 26519−26539

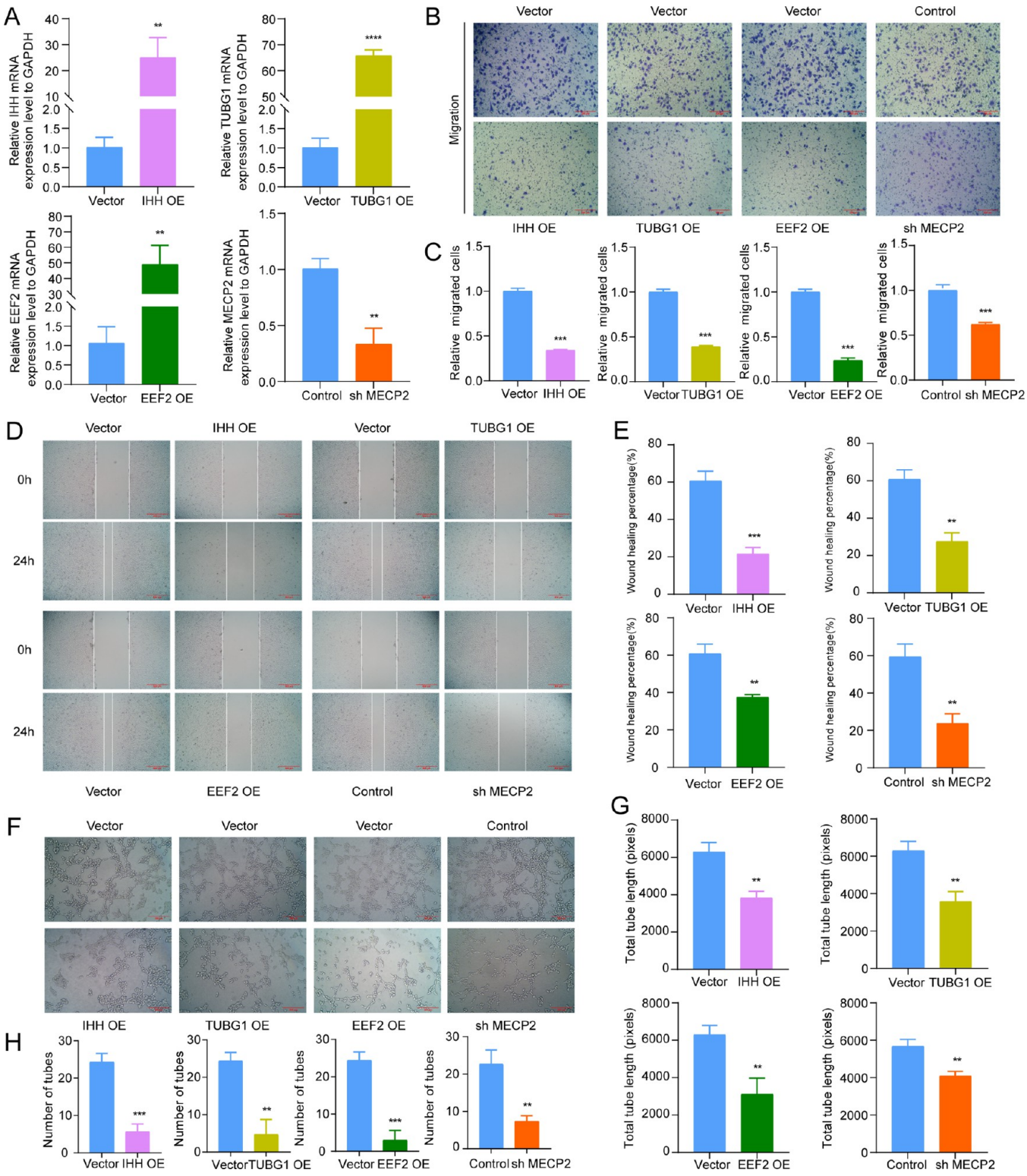

Figure 10. Selected angiogenesis-related hub genes regulated the migration and tube formation in vitro. (A) qRT-PCR analysis of IHH, TUBG1, and EEF2 overexpression and MECP2 knockdown efficiency. (B) Representative migration images of HUVECs cocultured with UCEC cells transfected with IHH, TUBG1, and EEF2 overexpression plasmids or MECP2 short hairpin RNA contrasted to vector or control in Transwell assays. (C) Bar graphs showed the statistics for cell counts. (D) Wound-Healing assays were performed in HUVECs cocultured with UCEC cells transfected with IHH, TUBG1 and EEF2 overexpression plasmids or MECP2 short hairpin RNA. Representative images at the indicated time points were shown (magnification ×4). (E) Quantitative analysis of the migration area was performed for HUVECs using ImageJ software. (F) Capillary tubule structures were represented for HUVECs treated with culture medium collected from the transfected UCEC cells by tube formation assays on Matrigel. Total tube length (G) and number of tubes(H) were calculated for individual treatment and expressed in pixel showing the angiogenic capacity of HUVECs transfected with the indicated constructs. *$P < 0.05$, **$P < 0.01$, ***$P < 0.001$, and ****$P < 0.0001$.

https://doi.org/10.1021/acsomega.4c03034
ACS Omega 2024, 9, 26519−26539

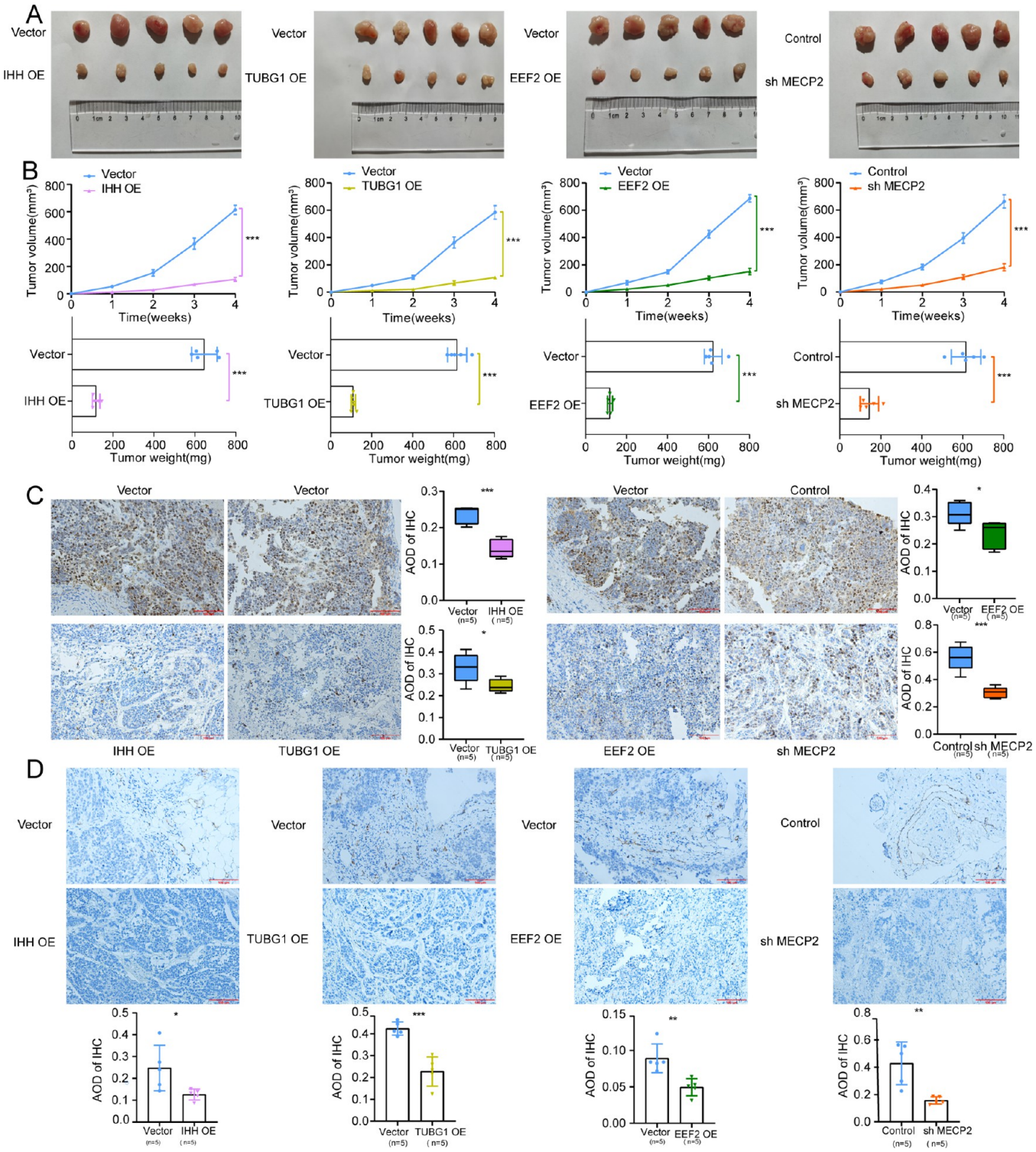

Figure 11. Selected angiogenesis-related hub genes affected tumor growth and angiogenesis in vivo. (A) Image of subcutaneous tumors formed in nude mice of HUVECs ($n = 5$). (B) Tumor volume and weight measurements in BALB/c nude mice. The relative protein levels of Ki67 (C) and CD31 (D) were determined in subcutaneous xenograft tumors by immunohistochemistry. *$P < 0.05$, **$P < 0.01$, and ***$P < 0.001$.

be inferred that the infiltration levels of immune and stromal cells improved along with the increase of APRS, given that APRS was markedly positively correlated with immune, stromal, and ESTIMATE scores but negatively correlated with tumor purity (Figure 8E).

3.7. Expression Levels of Selected Angiogenesis-Related Hub Genes. We tested the transcription levels of four angiogenesis-related hub genes (IHH, TUBG1, EEF2, and MECP2) involved in APRS in cell lines, UCEC tissues, and paratumor tissues. The results of qRT-PCR pointed out that the mRNA expression levels of IHH, TUBG1, and EEF2 in human UCEC cell lines showed an overall downward trend, yet the mRNA expression levels of MECP2 showed an overall upward trend compared with the human endometrial epithelial

https://doi.org/10.1021/acsomega.4c03034
ACS Omega 2024, 9, 26519−26539

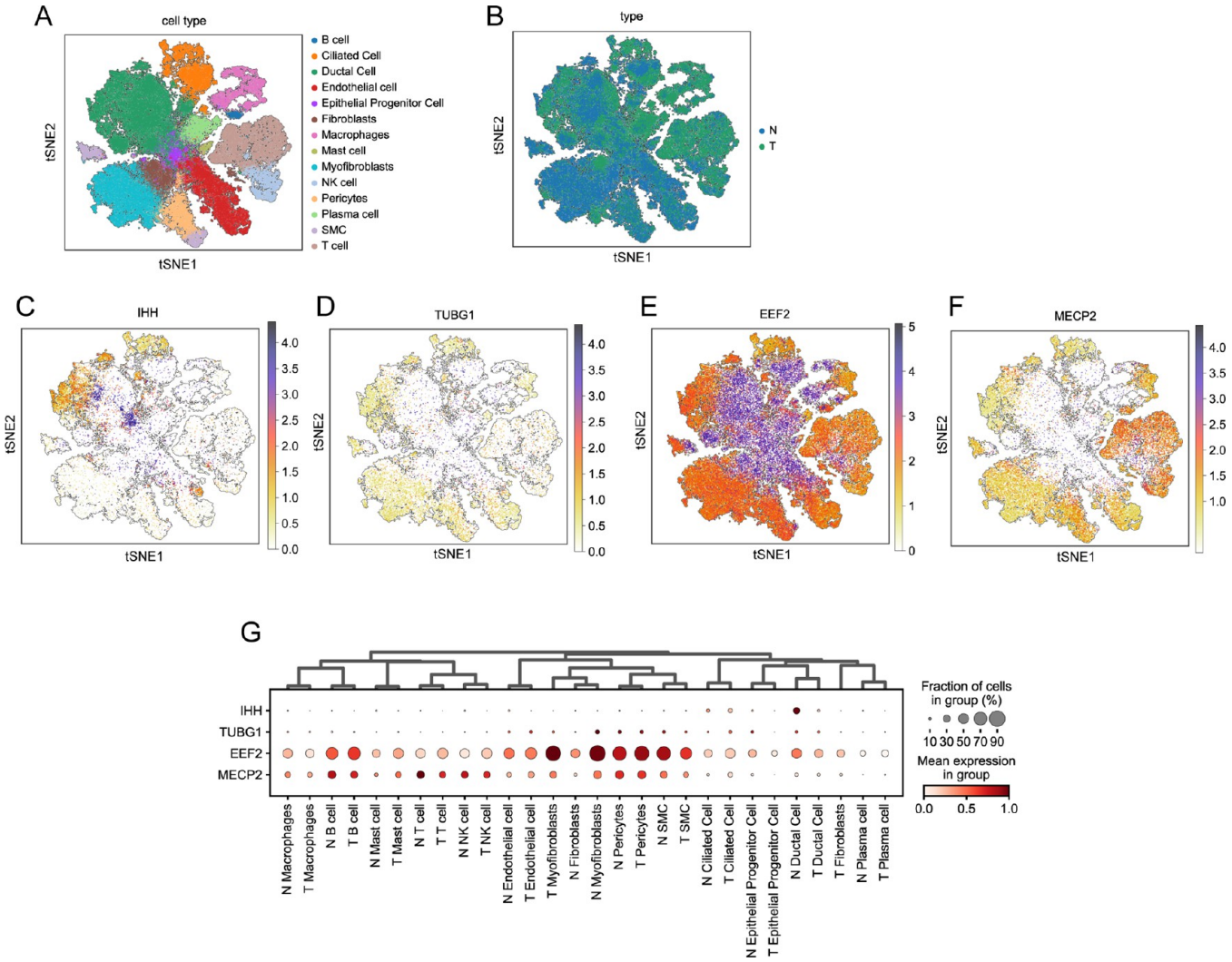

Figure 12. Single-cell sequencing validates endometrial cancer gene expression patterns. (A) Downscaled clustering plot of cell clusters. (B) Normal versus tumor tissue marker map. (C−F) Schematic diagram of gene distribution in different cell clusters. (G) Statistical dot plot of gene distribution in different cell clusters.

cells(hEECs) (Figure 9A). The qRT-PCR results of tissue samples were in accordance with those of cell lines. The transcription levels of IHH, TUBG1, and EEF2 in UCEC tissues decreased, while the transcription levels of MECP2 increased compared to adjacent tumor tissues (Figure 9B). In addition, the protein expression levels of these four angiogenesis-related prognostic hub genes were detected by IHC staining and analyzed by calculating the average optical density (AOD: IOD/area). Contrasted with paratumor tissues, IHH, TUBG1, and EEF2 were down-regulated in UCEC tissues, but up-regulated in MECP2 (Figure 9C). The representative IHC staining images are displayed in Figure 9D.

3.8. Selected Angiogenesis-Related Hub Genes Regulated the Migration and Tube Formation In Vitro. Research on gain- and loss-of-function was conducted to confirm the impact of selected angiogenesis-related hub genes on angiogenesis in UCEC. MECP2 shRNA was constructed and transfected into Ishikawa cells. IHH, TUBG1, and EEF2 overexpression plasmids were constructed and transfected into HEC-1B cells. The qRT-PCR results suggested the knockdown and overexpression efficiency (Figure 10A), and the CM was collected to treat HUVECs for subsequent functional experiments. Wound-Healing and Transwell assays revealed that IHH OE, TUBG1 OE, EEF2 OE, and sh MECP2 inhibited HUVEC migration (Figure 10B−E). The same trend was also reflected in the tube formation assay. IHH OE, TUBG1 OE, and EEF2 OE prominently suppressed tube formation in HUVECs as well as sh MECP2 (Figure 10F−H). In a word, MECP2 can promote the migration and tube formation of HUVECs in vitro. While IHH, TUBG1, and EEF2 have inhibitory effects.

3.9. Selected Angiogenesis-Related Hub Genes Affected Tumor Growth and Angiogenesis In Vivo. To gain further insights into the role of the selected angiogenesis-related hub genes in vivo, we subcutaneously injected the transfected UCEC cells and untreated UCEC cells as control into BALB/c-nu nude mice (5 weeks old) to establish a tumor xenograft model. Tumor-related indicators were measured weekly for 4 weeks until the mice were sacrificed and the tumors were removed. The weight and volume of tumors in IHH OE, TUBG1 OE, EEF2 OE, and shMECP2 were obviously smaller than those of the control group (Figure 11A,B). IHC staining of mouse tumor tissues showed that the expression levels of Ki67 were prominently downregulated in IHH OE, TUBG1 OE, EEF2 OE, and shMECP2 compared to the control group

https://doi.org/10.1021/acsomega.4c03034
ACS Omega 2024, 9, 26519−26539

(Figure 11C), and the same trend also existed in CD31 (Figure 11D). Overall, the above-mentioned results suggested that MECP2 acted on promoting the proliferation and angiogenesis of UCEC cells in vivo, while IHH, TUBG1, and EEF2 played an opposite role in vivo.

3.10. Single-Cell Sequencing Verified the Gene Features in Tumor Tissues. Following the elimination of low-quality cells, subsequent steps including normalization, dimensionality reduction, and integration resulted in the clustering of 99,215 cells into 14 clusters of cells identified by tagged genes to their origin (Figure 12A,B). Figure 12C−G illustrates the variations in gene expression levels of IHH, TUBG1, EEF2, and MECP2 in the 14 clusters of cells. Notably, the IHH gene exhibited high expression in ductal cells and ciliated cells, while TUBG1 was prominently expressed in myofibroblasts, pericytes, and epithelial progenitor cells. EEF2 gene displayed heightened expression levels in myofibroblasts, pericytes, and SMC clusters, and MECP2 was predominantly expressed in T cells, B cells, and NK cells.

4. DISCUSSION

Angiogenesis plays a major role in the development of cancer, from the beginning of carcinogenesis, the stage of carcinoma in situ to the late stage of cancer.[33] Excessive abnormal angiogenesis is instrumental in tumor progression. TIME is a new concept that has been reported to be closely related to the clinical prognosis of cancer patients.[34] Regulation between angiogenesis and the immune system is actually mutual; antiangiogenesis therapy and immunotherapy can also influence each other. In previous studies, VEGF-A/VEGFR-2 signaling pathway is generally considered to be the most important mechanism in angiogenesis.[35] Over the years, antiangiogenesis medicine has focused on targeting angiogenesis signal proteins, such as vascular endothelial growth factor (VEGF). Therefore, we believe that a comprehensive exploration of biomarkers related to angiogenesis is of great significance for identifying new tumor subtypes, predicting prognosis, and responding to immunotherapy. We employed the NMF algorithm to determine five angiogenic subtypes in 506 UCEC patients based on the expression profiles of 73 prognostic angiogenesis-related DEGs. Then, remarkable differences in prognosis, clinicopathological features, cancer hallmarks, genomic mutations, TIME patterns, and immunotherapy responses were observed among the five angiogenic subtypes. In order to carry out individualized comprehensive evaluation, a prognostic signature, APRS, was established by the WGCNA algorithm and LASSO Cox regression. It demonstrated the relationship between APRS and TIME patterns, genomic mutations, clinicopathological characteristics, and prognosis in patients with UCEC. The predictability of APRS for ICI treatment is also outstanding.

The top ten hallmarks of cancer currently comprise persistent proliferation signaling, evading growth inhibition, resistance to cell death, enabling replicative immortality, inducing angiogenesis, activating invasion and metastasis, genomic instability and mutation, promoting tumor inflammation, reprogramming energy metabolism, and avoiding immune destruction.[36] In pathological circumstances, it stimulates the host blood vessels' expansion to tumors in order to sustain cell proliferation. Vascular dilation, tortuosity, and disorder are characteristics of tumor angiogenesis.[37,38] Tumors continue to promote the growth of new blood vessels to ensure sufficient nutritional supply for expansion, which also provide potential pathways for tumor metastasis.[39] In recent years, many scientists have paid attention to the field of vascular development. Studies have revealed the process and mechanism by which vascular morphogenesis is regulated in development, physiology and pathology.[40] Ang1-induced Tie2 phosphorylation leads to AKT activation, thereby promoting the survival pathway of ECs, inhibiting the apoptotic pathway, and inactivating the forehead transcription factor (FOXO1).[41,42] TAK1 regulates MAPK signal transduction by activating P38 MAPK and JNK, promotes the expression of VEGF, plasminogen activator inhibitor-1 (PAI-1) and MMP, and participates in vascular remodeling, angiogenesis and ECM degradation in tumors such as glioma.[43,44] In the process of tumor angiogenesis, pod rosettes control vascular branches, in which VEGF stimulation induces tumor angiogenesis-related rosette formation by increasing $\alpha 6\beta 1$-integrin.[45] SHH induces PTCH1 and GLI1 to indirectly promote tumor angiogenesis, thereby inhibiting two abundant matrix-derived antiangiogenic factors (THBS2 and TIMP2), and directly promotes tumor angiogenesis by activating the small GTPase of the RHO family in the presence of VEGF.[46] In this study, different angiogenesis subtypes of UCEC patients showed conspicuous tumor hallmark characteristics quantified by ssGSEA. The EC1 subtype was associated with positive regulation of cell junctions and ECM, and the EC3 was positively correlated with many reputable cancer-related hallmarks, including metabolism, EMT, apoptosis, and inflammation, which echoed the active genomic mutation in EC1 and EC3. EC1 and EC3 displayed apparent malignant characteristics compared with EC2, EC4, and EC5, which afforded a possible explanation for the poor prognosis of EC1 and EC3. Otherwise, the constructed APRS also indicated a prominent correlation with these renowned tumor hallmarks. These results offered compelling evidence of the influence of angiogenesis in giving tumor-specific characteristics that cannot be ignored.

There is an intricate relationship between angiogenesis and immunity in tumors. More and more evidence suggests that immune system components play a key role in inducing cancer angiogenesis.[47−49]During the inflammatory response, immune cells synthesize and secrete proangiogenic factors, promoting the formation of new blood vessels. There is credible evidence that tumor-associated neutrophils (TAN) and their mediators are involved in tumor growth and progression, angiogenesis, and metastasis.[50−53] N2 neutrophils can promote tumor development by reshaping ECM, angiogenesis, and the production of pro-tumor cytokines and chemokines.[54−56] CD4 + T cells recruit and adhere to pericytes on endothelial blood vessels, promote vascular normalization through IFN-γ, and then coordinate the reprogramming of TIME by promoting Th1 T cell infiltration and reducing neutrophil inflow into the tumor microenvironment. On the other hand, the newly formed vascularity promotes the continuation of inflammation by promoting the migration of inflammatory cells to inflammatory sites.[57] For example, the normalization of the tumor vasculature by inhibiting VEGF has been shown to increase the infiltration of immune cells into tumors through a variety of mechanisms, including endothelial activation and subsequent increase in levels of cytokines and Th1 chemokines in tumors[58] and the reprogramming of macrophages from immunosuppressive to immunopermissive.[59−61] Angiogenesis and immune escape are considered biomarkers of cancer, typically occurring in parallel and interdependent processes. Both of these physiological mechanisms can be hijacked in cancer and promote the development and progression of tumors.[36,62] In this study,

https://doi.org/10.1021/acsomega.4c03034
ACS Omega 2024, 9, 26519−26539

EC1 and EC3 had higher immune scores and the lowest tumor purity compared to other subtypes, indicating that EC1 and EC3 were surrounded by more nontumor components. In addition, EC1 and EC3 displayed a higher infiltration of most immune cells than the other three subtypes. Therefore, it can be considered that EC1 and EC3 were in the immune inflammation mode and had a stronger immune function, which might reflect a better response to immunotherapy. The prediction of the ICI treatment response also confirmed the speculation. EC1 and EC3 presented significantly reduced TIDE scores, elevated MSI scores, and increased immune checkpoint expression levels. EC1 and EC3 may be more suitable for ICI treatment. In summary, this evidence suggested that the angiogenesis subtypes established in this study would be advantageous to the differential identification of TIME patterns and conducive to identifying patients suitable for ICI therapy.

In the past, UCEC was divided into type I and type II (Bokhman classification).[63] Type I was hormone-dependent, and the pathological type was predominantly endometrioid carcinoma, which had a better prognosis. Type II was nonhormone-dependent and had a dismal prognosis, consisting primarily of serous carcinoma, clear cell carcinoma, and carcinosarcoma. With the advancement of clinical research, immunotherapy and targeted therapy have also demonstrated good efficacy in the treatment of UCEC in recent years. Furthermore, widespread applications of gene detection provide more evidence for the diagnosis of UCEC, and also offer guidelines for the molecular subtypes and selection of targeted drugs of UCEC. In 2013, TCGA divided the patients of UCEC into four molecular types according to the characteristics of whole genome sequencing genes (with or without POLE gene hypermutation, MMR deletion, copy number variation, etc.).[64] ① POLE hypermutated type; ② MSI-H type (microsatellite instability) or mismatch repair-deficient type (dMMR); ③microsatellite stability (MSS) type or no-specific molecular profile (NSMP) type or low-copy type; ④ p53 mutation or high-copy type. In this study, with the largest percentage of MSS and the lowest percentage of MSI-H, the most frequently altered gene in the EC1 and EC3 subtypes was TP53, which was consistent with their poor survival rates. PTEN was the most common mutated gene in EC2, EC4, and EC5. Therefore, TP53 was considered to be a crucial predictive biomarker for UCEC. Although TP53 and PTEN mutation distribution varied with angiogenesis subtypes, we do not believe that the difference in survival among angiogenesis subtypes is due to the difference. It could be seen that the mutation rates of TP53 and PTEN in the EC3 subtype were similar, but the prognosis of EC3 was significantly worse than that of EC2, EC4, and EC5 subtypes. These findings illustrated the distinct features of the UCEC immune microenvironment and served as a helpful supplement for basic research.

In view of the multifaceted heterogeneity among the five angiogenic subtypes, we believed that it was viable to construct a risk score to quantify this heterogeneity and to individualized comprehensive assessments. The generated APRS, as expected, showed a strong ability to predict the prognosis and response to ICI therapy in addition to exhibiting a strong association with the clinicopathological characteristics, representative cancer hallmarks, genomic mutations, and TIME patterns of UCEC patients. Fourteen selected angiogenesis-related hub genes consisted of six protective genes and eight risk genes. MECP2, a methyl-CpG-binding protein, is increasingly being supported as a tumor activator in cancer development. In the majority of malignancies, MECP2 expression is connected with matrix score, immune score, and the quantity of immune cells, including T cell NK, Th1, M1, T cell CD4 + central memory, and dendritic cells.[65] MECP2 promoting the expression of HOXD3 through the HB-EGF cell signaling pathway induces migration, invasion, and angiogenesis of hepatocellular carcinoma.[66] IHH is expressed in the colon and prostate and inhibits the growth of colon cancer.[67,68] and prostate cancer.[69] As an antiangiogenic regulator, IHH pays tribute to the angiogenesis process.[70] There is a strong negative correlation between IHH and the methylation process, and their expression levels may be affected by epigenetic regulation, which can be a potential prognostic marker for UCEC patients.[71] TUBG1, as a microtubule protein, acts an essential role in microtubule formation.[72] In hepatocellular carcinoma, TUBG1 may be involved in ferroptosis-mediated tumor biological behavior through the hub gene FANCD2.[73] EEF2 is involved in the development and recurrence of tumors and has been found to be significantly expressed in a variety of cancers.[74] Furthermore, studies have shown that EEF2, a biomarker for human Achilles tendon regeneration, may improve autophagy, promote cell migration and proliferation, and lessen apoptosis and cell death in vivo.[75] The genes we screened are not ubiquitous in UCEC research. Whereas they are highly correlated with the malignant characteristics and prognosis of UCEC, which makes it of significant research significance. MECP2 has the ability to stimulate HUVEC migration and tube formation in vitro and in vivo tumor growth in mice. IHH, TUBG1, and EEF2 play the opposite role. At present, the research on these angiogenesis-related genes is almost entirely limited to the malignant phenotypes in which they participate. Therefore, it is necessary to investigate more in-depth mechanisms in the future, that is, how to influence the growth and occurrence of tumors, as a crucial aspect of angiogenesis.

Compared with the previous classification of UCEC patients, our study identified angiogenic subtypes in UCEC for the first time and constructed APRS, which demonstrated excellent diagnostic precision in predicting OS in patients with UCEC and held significant clinical translation value. In vivo and in vitro experiments have verified that MECP2 is a novel angiogenesis-related risk-regulatory factor for angiogenesis-related genes. Whereas, IHH, TUBG1 and EEF2 are protective genes. Our angiogenesis subtypes have the benefit of exhibiting multimodal heterogeneity, including variations in prognosis, clinicopathological features, cancer hallmarks, genomic mutations, TIME patterns, and immunotherapy responses, particularly the latter, which has significant clinical implications. Nevertheless, it is important to acknowledge a few of this study's weaknesses. First of all, the prognostic signature based on public databases is retrospective in nature, which means that additional prospective data will be required to verify and enhance its clinical utility. Second, the constrained database and small sample size of our study may contribute to a heightened likelihood of type I errors. Anticipated enhancements involving larger databases and expanded sample sizes are poised to better serve the research requirements of endometrial cancer scholars in forthcoming investigations. Concurrently, our research is limited to the presentation of malignant phenotypes and the expression verification of four representative genes, although combining bioinformatics analysis with in vitro and in vivo experiments. To validate the prognostic signatures, we will carry out comprehensive investigations of molecular mechanisms and clinical studies in the future.

https://doi.org/10.1021/acsomega.4c03034
ACS Omega 2024, 9, 26519−26539

5. CONCLUSIONS

In conclusion, five angiogenic subtypes with different prognosis, clinicopathological features, cancer hallmarks, genomic mutations, TIME patterns, and immunotherapy responses have been identified to distinguish and quantify the multidimensional heterogeneity of UCEC patients. A constructed prognostic signature, APRS, exhibited significant predictability in terms of prognosis and response to ICI therapy of UCEC.

■ ASSOCIATED CONTENT

Supporting Information

The Supporting Information is available free of charge at https://pubs.acs.org/doi/10.1021/acsomega.4c03034.

Association of angiogenic subtypes of UCEC in TCGA cohort; screening and functional enrichment analysis of angiogenesis-related hub genes; K-M curves of four representative genes and correlations of APRS with clinicopathological features (PDF)

Clinical features of tissues used for qRT-PCR and IHC; shRNA sequences and primers for qPCR; primary antibodies used in immunohistochemistry; transcriptome data of 531 differentially expressed UCEC-related genes obtained from TCGA cohort and GTEx database; total of 1550 angiogenesis-related genes obtained from AMIGO; 217 prognostic angiogenesis-related genes obtained by univariate Cox regression analysis; 73 prognostic angiogenesis-related DEGs of UCEC (XLSX)

■ AUTHOR INFORMATION

Corresponding Authors

Tangansu Zhang − *Department of Obstetrics and Gynecology, Union Hospital, Tongji Medical College, Huazhong University of Science and Technology, Wuhan 430022, China*; Email: zt_ansu@126.com

Hongbo Wang − *Department of Obstetrics and Gynecology, Union Hospital, Tongji Medical College, Huazhong University of Science and Technology, Wuhan 430022, China*; orcid.org/0000-0003-1591-297X; Email: drwanghb69@hust.edu.cn

Authors

Qi Zhang − *Department of Obstetrics and Gynecology, Union Hospital, Tongji Medical College, Huazhong University of Science and Technology, Wuhan 430022, China*

Yuwei Yao − *Department of Obstetrics and Gynecology, Union Hospital, Tongji Medical College, Huazhong University of Science and Technology, Wuhan 430022, China*

Zhicheng Yu − *Department of Obstetrics and Gynecology, The First Affiliated Hospital of USTC, Hefei 230001, China*

Ting Zhou − *Department of Obstetrics and Gynecology, Union Hospital, Tongji Medical College, Huazhong University of Science and Technology, Wuhan 430022, China*

Qian Zhang − *Department of Obstetrics and Gynecology, Union Hospital, Tongji Medical College, Huazhong University of Science and Technology, Wuhan 430022, China*

Haojia Li − *Department of Obstetrics and Gynecology, Union Hospital, Tongji Medical College, Huazhong University of Science and Technology, Wuhan 430022, China*

Jun Zhang − *Department of Obstetrics and Gynecology, Union Hospital, Tongji Medical College, Huazhong University of Science and Technology, Wuhan 430022, China*

Sitian Wei − *Department of Obstetrics and Gynecology, Sir Run Run Shaw Hospital, Zhejiang University School of Medicine, Hangzhou 310016, China*

Complete contact information is available at: https://pubs.acs.org/10.1021/acsomega.4c03034

Author Contributions

Formal analysis, writing−original draft, and writing−review and editing, Q.Z.; conceptualization and visualization, Y.Y.; data curation, Q.Z., T.Z., Q.Z., H.L., and S.W.; software and funding acquisition, Z.Y. and J.Z.; writing−review and editing and supervision, T.Z. and H.W. Qi Zhang and Yuwei Yao contributed equally to this paper.

Notes

The authors declare no competing financial interest.

■ ACKNOWLEDGMENTS

This study was supported by the Wuhan Knowledge Innovation Special project (NO. 2022020801010457).

■ REFERENCES

(1) Zhang, B.; Horvath, S. A General Framework for Weighted Gene Co-Expression Network Analysis. *Stat. Appl. Genet. Mol. Biol.* **2005**, *4*, 17.

(2) Chakraborty, S.; Njah, K.; Hong, W. Agrin Mediates Angiogenesis in the Tumor Microenvironment. *Trends Cancer* **2020**, *6* (2), 81−85.

(3) Kloepper, J.; Riedemann, L.; Amoozgar, Z.; Seano, G.; Susek, K.; Yu, V.; Dalvie, N.; Amelung, R. L.; Datta, M.; Song, J. W.; et al. Ang-2/VEGF Bispecific Antibody Reprograms Macrophages and Resident Microglia to Anti-Tumor Phenotype and Prolongs Glioblastoma Survival. *Proc. Natl. Acad. Sci. U. S. A.* **2016**, *113* (16), 4476−4481.

(4) Tartour, E.; Pere, H.; Maillere, B.; Terme, M.; Merillon, N.; Taieb, J.; Sandoval, F.; Quintin-Colonna, F.; Lacerda, K.; Karadimou, A.; et al. Angiogenesis and Immunity: A Bidirectional Link Potentially Relevant for the Monitoring of Antiangiogenic Therapy and the Development of Novel Therapeutic Combination with Immunotherapy. *Cancer Metastasis Rev.* **2011**, *30* (1), 83−95.

(5) Bamias, A.; Dimopoulos, M. A. Angiogenesis in Human Cancer: Implications in Cancer Therapy. *Eur. J. Int. Med.* **2003**, *14* (8), 459−469.

(6) Nossin, Y.; Farrell, E.; Koevoet, W. J. L. M.; Somoza, R. A.; Caplan, A. I.; Brachvogel, B.; van Osch, G. J. V. M. Angiogenic Potential of Tissue Engineered Cartilage From Human Mesenchymal Stem Cells Is Modulated by Indian Hedgehog and Serpin E1. *Front. Bioeng. Biotechnol.* **2020**, *8*, 327.

(7) Fagiani, E.; Christofori, G. Angiopoietins in Angiogenesis. *Cancer Lett.* **2013**, *328* (1), 18−26.

(8) Hack, S. P.; Zhu, A. X.; Wang, Y. Augmenting Anticancer Immunity Through Combined Targeting of Angiogenic and PD-1/PD-L1 Pathways: Challenges and Opportunities. *Front. Immunol.* **2020**, *11*, No. 598877.

(9) Wang, Y.; Zhang, Y.; Wang, F.; Li, T.; Song, X.; Shi, H.; Du, J.; Zhang, H.; Jing, H.; Han, J.; et al. Bioinformatics Analysis of Prognostic Value and Immunological Role of MeCP2 in Pan-Cancer. *Sci. Rep.* **2022**, *12*, 18518.

(10) Pulkkinen, H. H.; Kiema, M.; Lappalainen, J. P.; Toropainen, A.; Beter, M.; Tirronen, A.; Holappa, L.; Niskanen, H.; Kaikkonen, M. U.; Ylä-Herttuala, S.; et al. BMP6/TAZ-Hippo Signaling Modulates Angiogenesis and Endothelial Cell Response to VEGF. *Angiogenesis* **2021**, *24* (1), 129−144.

(11) He, Y.; Jiang, Z.; Chen, C.; Wang, X. Classification of Triple-Negative Breast Cancers Based on Immunogenomic Profiling. *J. Exp. Clin. Cancer Res. CR* **2018**, *37* (1), 327.

(12) Allen, E.; Jabouille, A.; Rivera, L. B.; Lodewijckx, I.; Missiaen, R.; Steri, V.; Feyen, K.; Tawney, J.; Hanahan, D.; Michael, I. P.; et al. Combined Antiangiogenic and Anti-PD-L1 Therapy Stimulates Tumor

Immunity through HEV Formation. *Sci. Transl. Med.* **2017**, *9* (385), No. eaak9679.
(13) Han, F.; Cao, D.; Zhu, X.; Shen, L.; Wu, J.; Chen, Y.; Xu, Y.; Xu, L.; Cheng, X.; Zhang, Y. Construction and Validation of a Prognostic Model for Hepatocellular Carcinoma: Inflammatory Ferroptosis and Mitochondrial Metabolism Indicate a Poor Prognosis. *Front. Oncol.* **2023**, *12*, No. 972434.
(14) Aguilar-Cazares, D.; Chavez-Dominguez, R.; Carlos-Reyes, A.; Lopez-Camarillo, C.; Hernadez de la Cruz, O. N.; Lopez-Gonzalez, J. S. Contribution of Angiogenesis to Inflammation and Cancer. *Front. Oncol.* **2019**, *9*, 1399.
(15) Lee, J. J.; Rothenberg, M. E.; Seeley, E. S.; Zimdahl, B.; Kawano, S.; Lu, W.-J.; Shin, K.; Sakata-Kato, T.; Chen, J. K.; Diehn, M.; et al. Control of Inflammation by Stromal Hedgehog Pathway Activation Restrains Colitis. *Proc. Natl. Acad. Sci. U. S. A.* **2016**, *113* (47), E7545−E7553.
(16) Augustin, H. G.; Koh, G. Y.; Thurston, G.; Alitalo, K. Control of Vascular Morphogenesis and Homeostasis through the Angiopoietin-Tie System. *Nat. Rev. Mol. Cell Biol.* **2009**, *10* (3), 165−177.
(17) Chung, A. S.; Ferrara, N. Developmental and Pathological Angiogenesis. *Annu. Rev. Cell Dev. Biol.* **2011**, *27*, 563−584.
(18) Schmittnaegel, M.; Rigamonti, N.; Kadioglu, E.; Cassará, A.; Wyser Rmili, C.; Kiialainen, A.; Kienast, Y.; Mueller, H.-J.; Ooi, C.-H.; Laoui, D.; et al. Dual Angiopoietin-2 and VEGFA Inhibition Elicits Antitumor Immunity That Is Enhanced by PD-1 Checkpoint Blockade. *Sci. Transl. Med.* **2017**, *9* (385), No. eaak9670.
(19) Peterson, T. E.; Kirkpatrick, N. D.; Huang, Y.; Farrar, C. T.; Marijt, K. A.; Kloepper, J.; Datta, M.; Amoozgar, Z.; Seano, G.; Jung, K.; et al. Dual Inhibition of Ang-2 and VEGF Receptors Normalizes Tumor Vasculature and Prolongs Survival in Glioblastoma by Altering Macrophages. *Proc. Natl. Acad. Sci. U. S. A.* **2016**, *113* (16), 4470−4475.
(20) Chen, J.; Wang, J.; Wu, X.; Simon, N.; Svensson, C. I.; Yuan, J.; Hart, D. A.; Ahmed, A. S.; Ackermann, P. W. eEF2 Improves Dense Connective Tissue Repair and Healing Outcome by Regulating Cellular Death, Autophagy, Apoptosis, Proliferation and Migration. *Cell. Mol. Life Sci.* **2023**, *80* (5), 128.
(21) Vitorino, P.; Meyer, T. Modular Control of Endothelial Sheet Migration. *Genes Dev.* **2008**, *22* (23), 3268−3281.
(22) Costa, G.; Harrington, K. I.; Lovegrove, H. E.; Page, D. J.; Chakravartula, S.; Bentley, K.; Herbert, S. P. Asymmetric Division Coordinates Collective Cell Migration in Angiogenesis. *Nat. Cell Biol.* **2016**, *18* (12), 1292−1301.
(23) Hamm, M. J.; Kirchmaier, B. C.; Herzog, W. Sema3d Controls Collective Endothelial Cell Migration by Distinct Mechanisms via Nrp1 and PlxnD1. *J. Cell Biol.* **2016**, *215* (3), 415−430.
(24) Haeger, A.; Wolf, K.; Zegers, M. M.; Friedl, P. Collective Cell Migration: Guidance Principles and Hierarchies. *Trends Cell Biol.* **2015**, *25* (9), 556−566.
(25) Sato, Y.; Rifkin, D. B. Inhibition of Endothelial Cell Movement by Pericytes and Smooth Muscle Cells: Activation of a Latent Transforming Growth Factor-Beta 1-like Molecule by Plasmin during Co-Culture. *J. Cell Biol.* **1989**, *109* (1), 309−315.
(26) Tchaikovski, V.; Olieslagers, S.; Böhmer, F.-D.; Waltenberger, J. Diabetes Mellitus Activates Signal Transduction Pathways Resulting in Vascular Endothelial Growth Factor Resistance of Human Monocytes. *Circulation* **2009**, *120* (2), 150−159.
(27) Kelley, M.; Fierstein, S.; Purkey, L.; DeCicco-Skinner, K. Endothelial Cell Tube Formation Assay: An In Vitro Model for Angiogenesis. In *VEGF Signaling: Methods and Protocols*; Fiedler, L. R.; Pellet-Many, C., Eds.; Springer US: New York, NY, 2022; pp 187−196.
(28) Ren, X.; Liang, J.; Zhang, Y.; Jiang, N.; Xu, Y.; Qiu, M.; Wang, Y.; Zhao, B.; Chen, X. Single-Cell Transcriptomic Analysis Highlights Origin and Pathological Process of Human Endometrioid Endometrial Carcinoma. *Nat. Commun.* **2022**, *13*, 6300.
(29) Kanugula, A. K.; Adapala, R. K.; Jamaiyar, A.; Lenkey, N.; Guarino, B. D.; Liedtke, W.; Yin, L.; Paruchuri, S.; Thodeti, C. K. Endothelial TRPV4 Channels Prevent Tumor Growth and Metastasis via Modulation of Tumor Angiogenesis and Vascular Integrity. *Angiogenesis* **2021**, *24* (3), 647−656.
(30) Shi, N.; Chen, X.; Liu, R.; Wang, D.; Su, M.; Wang, Q.; He, A.; Gu, H. Eukaryotic Elongation Factors 2 Promotes Tumor Cell Proliferation and Correlates with Poor Prognosis in Ovarian Cancer. *Tissue Cell* **2018**, *53*, 53−60.
(31) Bao, M.; Chen, Y.; Liu, J.-T.; Bao, H.; Wang, W.-B.; Qi, Y.-X.; Lv, F. Extracellular Matrix Stiffness Controls VEGF165 Secretion and Neuroblastoma Angiogenesis via the YAP/RUNX2/SRSF1 Axis. *Angiogenesis* **2022**, *25* (1), 71−86.
(32) Wu, Z.; Jeong, J.-H.; Ren, C.; Yang, L.; Ding, L.; Li, F.; Jiang, D.; Zhu, Y.; Lu, J. Fatty Acid-Binding Protein 4 (FABP4) Suppresses Proliferation and Migration of Endometrial Cancer Cells via PI3K/Akt Pathway. *OncoTargets Ther.* **2021**, *14*, 3929−3942.
(33) Mermel, C. H.; Schumacher, S. E.; Hill, B.; Meyerson, M. L.; Beroukhim, R.; Getz, G. GISTIC2.0 Facilitates Sensitive and Confident Localization of the Targets of Focal Somatic Copy-Number Alteration in Human Cancers. *Genome Biol.* **2011**, *12* (4), R41.
(34) Sung, H.; Ferlay, J.; Siegel, R. L.; Laversanne, M.; Soerjomataram, I.; Jemal, A.; Bray, F. Global Cancer Statistics 2020: GLOBOCAN Estimates of Incidence and Mortality Worldwide for 36 Cancers in 185 Countries. *CA. Cancer J. Clin.* **2021**, *71* (3), 209−249.
(35) Loffredo, S.; Borriello, F.; Iannone, R.; Ferrara, A. L.; Galdiero, M. R.; Gigantino, V.; Esposito, P.; Varricchi, G.; Lambeau, G.; Cassatella, M. A.; et al. Group V Secreted Phospholipase A2 Induces the Release of Proangiogenic and Antiangiogenic Factors by Human Neutrophils. *Front. Immunol.* **2017**, *8*, 443.
(36) Hanahan, D.; Weinberg, R. A. Hallmarks of Cancer: The next Generation. *Cell* **2011**, *144* (5), 646−674.
(37) Bausch, D.; Fritz, S.; Bolm, L.; Wellner, U. F.; Fernandez-Del-Castillo, C.; Warshaw, A. L.; Thayer, S. P.; Liss, A. S. Hedgehog Signaling Promotes Angiogenesis Directly and Indirectly in Pancreatic Cancer. *Angiogenesis* **2020**, *23* (3), 479−492.
(38) Iasonos, A.; Schrag, D.; Raj, G. V.; Panageas, K. S. How to Build and Interpret a Nomogram for Cancer Prognosis. *J. Clin. Oncol. Off. J. Am. Soc. Clin. Oncol.* **2008**, *26* (8), 1364−1370.
(39) Shen, R.; Li, P.; Li, B.; Zhang, B.; Feng, L.; Cheng, S. Identification of Distinct Immune Subtypes in Colorectal Cancer Based on the Stromal Compartment. *Front. Oncol.* **2020**, *9*, 1497.
(40) Khan, K. A.; Kerbel, R. S. Improving Immunotherapy Outcomes with Anti-Angiogenic Treatments and Vice Versa. *Nat. Rev. Clin. Oncol.* **2018**, *15* (5), 310−324.
(41) Yoshihara, K.; Shahmoradgoli, M.; Martínez, E.; Vegesna, R.; Kim, H.; Torres-Garcia, W.; Treviño, V.; Shen, H.; Laird, P. W.; Levine, D. A.; et al. Inferring Tumour Purity and Stromal and Immune Cell Admixture from Expression Data. *Nat. Commun.* **2013**, *4*, 2612.
(42) Cancer Genome Atlas Research Network; Kandoth, C.; Schultz, N.; Cherniack, A. D.; Akbani, R.; Liu, Y.; Shen, H.; Robertson, A. G.; Pashtan, I.; Shen, R.; et al. Integrated Genomic Characterization of Endometrial Carcinoma. *Nature* **2013**, *497* (7447), 67−73.
(43) Zhong, Q.; Fan, J.; Chu, H.; Pang, M.; Li, J.; Fan, Y.; Liu, P.; Wu, C.; Qiao, J.; Li, R.; et al. Integrative Analysis of Genomic and Epigenetic Regulation of Endometrial Cancer. *Aging* **2020**, *12* (10), 9260−9274.
(44) Mayakonda, A.; Lin, D.-C.; Assenov, Y.; Plass, C.; Koeffler, H. P. Maftools: Efficient and Comprehensive Analysis of Somatic Variants in Cancer. *Genome Res.* **2018**, *28* (11), 1747−1756.
(45) Risau, W. Mechanisms of Angiogenesis. *Nature* **1997**, *386* (6626), 671−674.
(46) Wang, L.; Gao, Y.; Tong, D.; Wang, X.; Guo, C.; Guo, B.; Yang, Y.; Zhao, L.; Zhang, J.; Yang, J.; et al. MeCP2 Drives Hepatocellular Carcinoma Progression via Enforcing HOXD3 Promoter Methylation and Expression through the HB-EGF/EGFR Pathway. *Mol. Oncol.* **2021**, *15* (11), 3147−3163.
(47) Carmeliet, P.; Jain, R. K. Molecular Mechanisms and Clinical Applications of Angiogenesis. *Nature* **2011**, *473* (7347), 298−307.
(48) Tian, L.; Goldstein, A.; Wang, H.; Ching Lo, H.; Sun Kim, I.; Welte, T.; Sheng, K.; Dobrolecki, L. E.; Zhang, X.; Putluri, N.; et al. Mutual Regulation of Tumour Vessel Normalization and Immunostimulatory Reprogramming. *Nature* **2017**, *544* (7649), 250−254.

https://doi.org/10.1021/acsomega.4c03034
ACS Omega 2024, 9, 26519−26539

(49) Mantovani, A.; Cassatella, M. A.; Costantini, C.; Jaillon, S. Neutrophils in the Activation and Regulation of Innate and Adaptive Immunity. *Nat. Rev. Immunol.* **2011**, *11* (8), 519−531.
(50) Jablonska, J.; Leschner, S.; Westphal, K.; Lienenklaus, S.; Weiss, S. Neutrophils Responsive to Endogenous IFN-Beta Regulate Tumor Angiogenesis and Growth in a Mouse Tumor Model. *J. Clin. Invest.* **2010**, *120* (4), 1151−1164.
(51) de Visser, K. E.; Eichten, A.; Coussens, L. M. Paradoxical Roles of the Immune System during Cancer Development. *Nat. Rev. Cancer* **2006**, *6* (1), 24−37.
(52) Seano, G.; Daubon, T.; Génot, E.; Primo, L. Podosomes as Novel Players in Endothelial Biology. *Eur. J. Cell Biol.* **2014**, *93* (10−12), 405−412.
(53) Fridlender, Z. G.; Sun, J.; Kim, S.; Kapoor, V.; Cheng, G.; Ling, L.; Worthen, G. S.; Albelda, S. M. Polarization of Tumor-Associated Neutrophil Phenotype by TGF-Beta: "N1" versus "N2" TAN. *Cancer Cell* **2009**, *16* (3), 183−194.
(54) Chen, B.; Khodadoust, M. S.; Liu, C. L.; Newman, A. M.; Alizadeh, A. A. Profiling Tumor Infiltrating Immune Cells with CIBERSORT. *Methods Mol. Biol. Clifton NJ.* **2018**, *1711*, 243−259.
(55) Kaminska, B.; Cyranowski, S. Recent Advances in Understanding Mechanisms of TGF Beta Signaling and Its Role in Glioma Pathogenesis. *Adv. Exp. Med. Biol.* **2020**, *1202*, 179−201.
(56) Chen, Z.; Zhou, L.; Liu, L.; Hou, Y.; Xiong, M.; Yang, Y.; Hu, J.; Chen, K. Single-Cell RNA Sequencing Highlights the Role of Inflammatory Cancer-Associated Fibroblasts in Bladder Urothelial Carcinoma. *Nat. Commun.* **2020**, *11* (1), 5077.
(57) Yang, Z.; Peng, Y.-C.; Gopalan, A.; Gao, D.; Chen, Y.; Joyner, A. L. Stromal Hedgehog Signaling Maintains Smooth Muscle and Hampers Micro-Invasive Prostate Cancer. *Dis. Model. Mech.* **2016**, *10* (1), 39−52.
(58) Gerling, M.; Büller, N. V. J. A.; Kirn, L. M.; Joost, S.; Frings, O.; Englert, B.; Bergström, Å.; Kuiper, R. V.; Blaas, L.; Wielenga, M. C. B.; et al. Stromal Hedgehog Signalling Is Downregulated in Colon Cancer and Its Restoration Restrains Tumour Growth. *Nat. Commun.* **2016**, *7*, 12321.
(59) Huang, H.; Bhat, A.; Woodnutt, G.; Lappe, R. Targeting the ANGPT-TIE2 Pathway in Malignancy. *Nat. Rev. Cancer* **2010**, *10* (8), 575−585.
(60) Kaminska, B.; Kocyk, M.; Kijewska, M. TGF Beta Signaling and Its Role in Glioma Pathogenesis. *Adv. Exp. Med. Biol.* **2013**, *986*, 171−187.
(61) Baeriswyl, V.; Christofori, G. The Angiogenic Switch in Carcinogenesis. *Semin. Cancer Biol.* **2009**, *19* (5), 329−337.
(62) Carnevale, S.; Ghasemi, S.; Rigatelli, A.; Jaillon, S. The Complexity of Neutrophils in Health and Disease: Focus on Cancer. *Semin. Immunol.* **2020**, *48*, No. 101409.
(63) Delprat, V.; Huart, C.; Feron, O.; Soncin, F.; Michiels, C. The Impact of Macrophages on Endothelial Cells Is Potentiated by Cycling Hypoxia: Enhanced Tumor Inflammation and Metastasis. *Front. Oncol.* **2022**, *12*, No. 961753.
(64) Murdoch, C.; Muthana, M.; Coffelt, S. B.; Lewis, C. E. The Role of Myeloid Cells in the Promotion of Tumour Angiogenesis. *Nat. Rev. Cancer* **2008**, *8* (8), 618−631.
(65) Viallard, C.; Larrivée, B. Tumor Angiogenesis and Vascular Normalization: Alternative Therapeutic Targets. *Angiogenesis* **2017**, *20* (4), 409−426.
(66) Galdiero, M. R.; Garlanda, C.; Jaillon, S.; Marone, G.; Mantovani, A. Tumor Associated Macrophages and Neutrophils in Tumor Progression. *J. Cell. Physiol.* **2013**, *228* (7), 1404−1412.
(67) Albini, A.; Tosetti, F.; Benelli, R.; Noonan, D. M. Tumor Inflammatory Angiogenesis and Its Chemoprevention. *Cancer Res.* **2005**, *65* (23), 10637−10641.
(68) Bergers, G.; Benjamin, L. E. Tumorigenesis and the Angiogenic Switch. *Nat. Rev. Cancer* **2003**, *3* (6), 401−410.
(69) Shaul, M. E.; Fridlender, Z. G. Tumour-Associated Neutrophils in Patients with Cancer. *Nat. Rev. Clin. Oncol.* **2019**, *16* (10), 601−620.
(70) Bokhman, J. V. Two Pathogenetic Types of Endometrial Carcinoma. *Gynecol. Oncol.* **1983**, *15* (1), 10−17.
(71) Huang, Y.; Yuan, J.; Righi, E.; Kamoun, W. S.; Ancukiewicz, M.; Nezivar, J.; Santosuosso, M.; Martin, J. D.; Martin, M. R.; Vianello, F.; et al. Vascular Normalizing Doses of Antiangiogenic Treatment Reprogram the Immunosuppressive Tumor Microenvironment and Enhance Immunotherapy. *Proc. Natl. Acad. Sci. U. S. A.* **2012**, *109* (43), 17561−17566.
(72) Ellis, L. M.; Hicklin, D. J. VEGF-Targeted Therapy: Mechanisms of Anti-Tumour Activity. *Nat. Rev. Cancer* **2008**, *8* (8), 579−591.
(73) Langfelder, P.; Horvath, S. WGCNA: An R Package for Weighted Correlation Network Analysis. *BMC Bioinformatics* **2008**, *9*, 559.
(74) Wang, J.; Song, T.; Zhou, S.; Kong, X. YAP Promotes the Malignancy of Endometrial Cancer Cells via Regulation of IL-6 and IL-11. *Mol. Med. Camb. Mass* **2019**, *25* (1), 32.
(75) Mukherjee, A.; Conduit, P. T. γ-TuRCs. *Curr. Biol. CB* **2019**, *29* (11), R398−R400.

https://doi.org/10.1021/acsomega.4c03034
ACS Omega 2024, 9, 26519−26539